

# Assessing Exposures to Particulate Matter and Manganese in Welding Fumes

by

Sa Liu

A dissertation submitted in partial satisfaction of the

requirements for the degree of

Doctor of Philosophy

in

Environmental Health Sciences

in the

Graduate Division

of the

University of California, Berkeley

Committee in charge:

Professor S. Katharine Hammond, Chair

Professor Alan Hubbard

Professor John R. Balmes

Fall 2010

UMI Number: 3449005

All rights reserved

INFORMATION TO ALL USERS

The quality of this reproduction is dependent upon the quality of the copy submitted.

In the unlikely event that the author did not send a complete manuscript and there are missing pages, these will be noted. Also, if material had to be removed, a note will indicate the deletion.



UMI 3449005

Copyright 2011 by ProQuest LLC.

All rights reserved. This edition of the work is protected against unauthorized copying under Title 17, United States Code.



ProQuest LLC  
789 East Eisenhower Parkway  
P.O. Box 1346  
Ann Arbor, MI 48106-1346



This doctoral dissertation is dedicated to Dr. Qiuyuan Liu, for his wisdom, intellect, optimism, love and support, and to Ms. Juanxia Li, for her love, great support and being with me through this challenge.

## Acknowledgement

I express my deepest gratitude to Professor S. Katharine Hammond, my academic advisor and Chair of my dissertation committee, for her accepting me as her student to work with and learn from her and bringing me into the field of exposure assessment and occupational health; for her guidance through challenges in research along the way; for her encouragement and support during difficult times. Professor Hammond's meticulous work style deeply inspires me. Professor Hammond is also a committed enthusiastic mentor. Through working with her, I learnt not only how to think scientifically, but also how to work effectively in the academic world. I attribute my achievements to the great mentorship of Professor Hammond.

Special thanks goes to Professor Stephen M. Rappaport, for providing access to welding fume exposure database and for his guidance through statistical analysis of the data. I thank Professor Alan Hubbard for his suggestions on evaluating variable importance, testing interactions and presenting modeling results. I also want to thank Professor John R. Balmes for his comments during graduate group examination, qualify examination and in the final stage of dissertation revising. I particularly thank Professor Robert C. Spear for chairing my examination committees and providing comments on the significance of the projects to the field of occupational and environmental health sciences. I express my special thanks to Professor Mark Nicas for his invaluable technical help in mathematical modeling and encouragement. Special thanks also goes to Elizabeth Marianne Noth for many discussions on details in statistical modeling. These discussions clarified many confusing issues in a timely manner.

The work conducted in this dissertation was supported by NIOSH Education and Research Center/Northern California Center for Occupational and Environmental Health (NIOSH ERC Grant No. T42 OH 008429-02), a joint funding from management of an automobile facility and United Auto Workers (UAW) Local, and Suzanne Llewellyn Student Award from Center for Occupational and Environmental Health at UC Berkeley. Particular thanks are given to the funding agencies and organizations. During the particle mapping study in the automobile assembly plant, Hank J. McDermott provided invaluable comments on ventilation from engineering aspects; students from UC Berkeley *PH267 Characterization of Airborne Chemicals Class 2005* collected partial preliminary data. I wish to thank Hank J. McDermott, students from the class, as well as the union, the management and the workers at the plant for their assistance.

For the project conducted in three Chinese factories, my deep gratitude goes to my friend Mr. Jianlin Lu and his colleagues, for their assistance in obtaining access to the factories, and for Jianlin's help on daily accommodation, transportation, and coordination with the management of the factories. My deep gratitude also goes to Jenna Hua, an undergraduate student in Nutrition at UC Berkeley at the time and a graduate student in Environmental Health Sciences now, for her partnership and hard work during data collection in the factories. I also appreciate the cooperation of the factories and the workers who permitted their exposures to be measured.

At the last but not the least, I would like to thank my wonderful daughter, Longchao Liu, and son, Roy Liu, for their understanding, and for the happiness they bring to me every day.

# Table of Contents

Dedication.....	i
Acknowledgements.....	ii
Table of Contents.....	iii
List of symbols.....	vi
Abstract.....	1
Chapter 1: Introduction	
Section 1: History of welding.....	1
Section 2: Welding processes.....	2
Section 3: Health hazards in welding.....	3
Section 4: Manganese and welding.....	4
Section 5: Work in this dissertation.....	5
References.....	6
Chapter 2: Application of mixed models to assess welding exposures to total particulate matter and manganese	
Section 1: Introduction.....	8
Section 2: Methods.....	8
Section 2.1: Data compilation.....	8
Section 2.2: Statistical modeling.....	9
Section 3: Results.....	11
Section 3.1: Descriptive analysis.....	11
Section 3.2: Statistical modeling.....	12
Section 4: Discussion.....	13
Section 4.1: Exposure determinants.....	13
Section 4.2: Exposure levels.....	14
Section 4.3: Controlling exposures to welding fumes.....	15
References.....	16
Figures.....	18
Tables.....	19
Chapter 3: Mapping particulate matter at the body weld department in an automobile assembly plant	
Section 1: Introduction.....	33

Section 2: Methods.....	34
Section 2.1: Facility/Process description.....	34
Section 2.2: Sampling instruments.....	35
Section 2.3: Data collection.....	36
Section 2.4: Map generation.....	36
Section 2.5: Statistical analysis.....	37
Section 3: Results.....	37
Section 3.1: Mapping method development.....	37
Section 3.1.1: Short-term variation and sampling interval.....	37
Section 3.1.2: Temporal variation during a shift.....	38
Section 3.2: Mapping results.....	39
Section 3.2.1: Spatial variations.....	39
Section 3.2.2: Day-to-day variations of the spatial distribution.....	40
Section 3.2.3: Particle size distributions.....	40
Section 4: Discussion.....	40
Section 4.1: Temporal variations and mapping implications.....	41
Section 4.2: Variation of spatial average and evaluation of reduction.....	41
Section 4.3: Spatial variations and ventilation conditions.....	42
Section 4.4: Particle size distributions.....	43
Section 5: Conclusions.....	43
References.....	45
Figures.....	46
Tables.....	53

Chapter 4: Manganese exposure and size distribution in welding fumes in three Chinese factories

Section 1: Introduction.....	57
Section 2: Methods.....	58
Section 2.1: Identifying welding processes and facilities.....	58
Section 2.2: Sampling instruments.....	59
Section 2.3: Data collection.....	59
Section 2.4: Analytical method.....	60
Section 3: Results.....	60
Section 3.1: Particle and manganese exposure levels.....	60
Section 3.2: Particle size distribution .....	61

Section 3.3: Manganese size distribution.....	61
Section 4: Discussion.....	61
Section 4.1: Exposure levels.....	61
Section 4.2: Manganese size distribution.....	62
Section 4.3: Effects of process and material.....	62
Section 5: Future steps.....	63
References.....	64
Figures.....	65
Tables.....	69
Chapter 5: Conclusions	
Conclusions.....	76
Further steps.....	79

## List of Symbols

ACGIH: American Conference of Governmental Industrial Hygienists

AM: arithmetic mean

ATSDR: Agency for Toxic Substances and Disease Registry

AWS: American welding society

FCAW: flux cored arc welding

GM: geometric mean

GSD: geometric standard deviation

GMAW: Gas metal arc welding

GTAW: gas tungsten arc welding

IARC: International Agency for Research on Cancer

LEV: local-exhaust ventilation

LOD: limit of detection

MCE: mixed cellular ester filter

MIG: metal inert gas

MMA: manual arc welding

Mn: manganese

NIOSH: National Institute for Occupational Safety and Health

OEL: occupational exposure limit

OSHA: Occupational Safety and Health Administration

PAW: plasma arc welding

PEL: permissible exposure limit

PM: particulate matter

PTFE: polytetrafluoroethylene

SAW: submerged arc welding

SD: standard deviation

SMAW: shielded metal arc welding

TIG: tungsten inert gas

TLV: threshold limit value

TP: total particulate matter

## Abstract

### Assessing Exposures to Particulate Matter and Manganese in Welding Fumes

By

Sa Liu

Doctor of Philosophy in Environmental Health Sciences

University of California, Berkeley

Professor S. Katharine Hammond, Chair

Linear mixed models were used to analyze data compiled from international sources to simultaneously estimate the fixed effects, associated with process characteristics and sampling regimen, and the variance components, associated with the random effects. The fixed effects explained 55% and 49% of variation in TP and Mn exposures, respectively. The country, industry/trade, ventilation condition, type of work/welding process, and material employed appeared to be the major factors affecting exposures to TP and Mn. Measurements in the U.S. were generally higher than those in other countries. Exposure to TP was 64% higher in enclosed spaces and 42% lower with local exhaust ventilation, was higher among boiler makers, and was higher when a mild-steel base metal was used. Exposure to Mn was 318% higher in enclosed spaces and 67% lower when local exhaust ventilation was present. The measured Mn air concentration was significantly related to the composition of the consumables, but not to the base metal. Resistance welding produced significantly lower TP and Mn exposures compared to other welding processes. After controlling for fixed effects, variance components between groups and between individual workers within a group were reduced by 89% and 57% for TP, and 75% and 63% for Mn, respectively. The within-worker variance component in Mn exposure was three times higher than that of TP, indicating that day-to-day and within-day variations in TP and Mn exposures were influenced by different factors that were not captured equally well by the mixed models for these two contaminants. Interestingly, exposures to TP and Mn had not changed over the 40 years of observation. The estimated probabilities of exceeding occupational exposure limits were very high (generally much greater than 10%) for both agents. Welding exposures to TP and Mn vary considerably across the world and across occupational groups. Exposures to both contaminants have been and continue to be unacceptably high in most sectors of industry. Because exposures to the two agents have different determinants, separate control strategies should be used for reducing welders' exposures to TP and Mn.

A respiratory health survey conducted in an automobile assembly plant in 2000-2001 found that welders had elevated rates of self-reported respiratory symptoms compared to painters and assembly workers. Subsequently, the ventilation system was improved at the body weld

department. In a follow-up study, particle spatial distributions were analyzed, following a mapping protocol developed specifically for this work place, to evaluate the effectiveness of the changes. Significant temporal and spatial variations were observed. Temporal variation during a shift was monitored with over-shift stationary sampling at fixed locations. Spatial variation was evaluated with 1-minute time-weighted average particle concentrations measured throughout the process areas (212 locations). The arithmetic spatial mean across 212 locations for the respirable particles varied from  $305\mu\text{g}/\text{m}^3$  to  $501\mu\text{g}/\text{m}^3$  on six sampled days, with a standard deviation of  $71\mu\text{g}/\text{m}^3$ , indicating that the difference between before and after countermeasures must be at least  $191\mu\text{g}/\text{m}^3$  in order to be considered statistically significant at the given sample sizes. The available data were not sufficient to evaluate the reduction of the particle concentrations after the countermeasures. The map of particle mass concentration revealed several high concentration areas, requiring further investigation and potentially higher level of controls. Resistance welding needed to be effectively controlled as it could be the major particle emitting source in the facility. The map of submicrometer ( $0.014\mu\text{m}$  to  $1.0\mu\text{m}$ ) particle count concentration presented different patterns from that of respirable particle mass concentration, indicating that the submicrometer particles tended to be more evenly distributed over the process areas. Workers not in close proximity to intensive welding operations might be exposed to fine particles at levels higher than had traditionally been thought. Mapping was demonstrated to be an effective method to assess particle spatial distributions. A well-designed sampling protocol is critical in order to achieve the specific aims of a mapping study.

A pilot study was conducted in three Chinese manufacturing facilities to characterize welders' exposure to particulate matter (PM) and airborne manganese (Mn) from common welding processes, with emphasis on Mn distribution in submicrometer particles. Particle air concentration was measured as 8-hour time-weighted averages (TWAs) for total and respirable particles. Mn air concentration (8hr TWA) was measured as Mn in total and respirable particles. Mn size distribution was assessed using multi-stage impactors with cut-points of  $0.25\mu\text{m}$ ,  $0.5\mu\text{m}$ ,  $1.0\mu\text{m}$  and  $2.5\mu\text{m}$ . The welding processes investigated were shielded metal arc welding, gas metal arc welding, submerged arc welding and plasma arc welding. Overall arithmetic means (AMs) across processes and factories were  $2.58\text{ mg}/\text{m}^3$  (range:  $0.338\text{ mg}/\text{m}^3 - 27.8\text{ mg}/\text{m}^3$ , GM:  $1.28\text{ mg}/\text{m}^3$ , GSD: 3.27) and  $1.46\text{ mg}/\text{m}^3$  (range:  $0.011\text{ mg}/\text{m}^3 - 14.7\text{ mg}/\text{m}^3$ , GM:  $0.698\text{ mg}/\text{m}^3$ , GSD: 3.37) for total and respirable particles (8hr TWAs), respectively. Overall AMs for Mn air concentrations were  $0.122\text{ mg}/\text{m}^3$  (range:  $0.001\text{ mg}/\text{m}^3 - 1.30\text{ mg}/\text{m}^3$ , GM:  $0.058\text{ mg}/\text{m}^3$ , GSD: 3.40) and  $0.073\text{ mg}/\text{m}^3$  (range:  $0.001\text{ mg}/\text{m}^3 - 0.650\text{ mg}/\text{m}^3$ , GM:  $0.036\text{ mg}/\text{m}^3$ , GSD: 3.33) for Mn in total and respirable particles, respectively. Particle and Mn concentrations varied over 4-fold by process. Shielded metal arc welding produced higher air concentrations for both agents compared to gas metal arc welding and submerged arc welding. Plasma arc welding resulted in the lowest concentrations. Manganese was found to be more concentrated in respirable particles than in total particles. Four percent of the particle mass of total particles was composed of Mn, while it was 5% for respirable particles. Data from the multi-stage impactor further revealed that majority of Mn mass, 97% for plasma arc welding and over 85% for shielded metal arc welding and gas metal arc welding, was distributed in particles smaller than  $0.5\mu\text{m}$ . Percentage of particle mass made of by Mn increased three to twenty times as particle size decreased from  $2.5\mu\text{m}$  –  $10\mu\text{m}$  to  $<0.25\mu\text{m}$ . These findings are of great significance in that Mn primarily targets the

central nervous system and Mn in small particles in the nano-size range has higher potential to reach the brain than Mn in larger particles. Therefore, welders' risk of developing neurological effects due to exposures to Mn may be higher than it had been traditionally thought. It was also observed that Mn size distribution varied by processes. Plasma arc welding and gas metal arc welding could be more hazardous than submerged arc welding when particle and Mn air concentrations are comparable. Shielded metal arc welding should be evaluated and controlled with high priority.

# Chapter 1: Introduction

## History of welding

Human history of welding can be traced back to ancient times. The earliest examples come from the Bronze Age. A gold bowl found in the tomb of Queen Pu-abi (~ 3000BC, queen of the Sumerian city of Ur, which is modern Iraq) had a wire twisted handle brazed to the outside wall. In about the same time period, the Egyptians used charcoal fires to heat iron ore to reduce it to sponge iron, and then welded the particles together by hammering. This was the first recorded welding process, known as “forge welding”, a method to join iron and steel by heating and hammering them. Small gold circular boxes assembled by forge-welded lapped joints were discovered in Roscommon, Ireland. These boxes were made more than 2000 years ago. During the Iron Age, the Egyptians and people in the eastern Mediterranean area used forge welding to weld iron pieces together. Many iron and bronze tools and items, found in the excavations near the pyramids in Egypt, were forge-welded in approximately 1000 B.C. During the Middle Ages, the art of blacksmithing was developed and many items of iron were produced by hammering. Forge welding remained the only welding process used for centuries until the end of the 19th century, when the modern welding technology, as we know it today, was developed (Cary and Helzer, 2004; Sapp, 2009).

Arc welding and oxyfuel welding were the first processes developed late in the 19<sup>th</sup> century, and resistance welding followed soon after. Generating electrical arc between two carbon electrodes using a battery was first demonstrated by Sir Humphrey Davy of London England in 1801. Following the invention of electric generator in the mid-nineteenth century, arc welding with the carbon electrodes and metal electrodes was developed. In 1881-82 a Russian inventor Nikolai Benardos created the first electric arc welding method known as carbon arc welding. The method was termed “*Electrohefest*” in memory of *Hephaestus*, the ancient Greek god of fire and blacksmith work, who gives instruction to the craftsmen forging metal. Metal electrodes were invented in the late 1800s. In 1890, C.L. Coffin of Detroit was awarded the first U.S. patent for an arc welding process using a metal electrode. This was the first record of the metal melted from the electrode carried across the arc to deposit filler metal in the joint to make a weld (Sapp, 2009).

Acetylene was first discovered by Edmund Davy of England in 1836. John Motley Morehead, a graduate of North Carolina State University in 1891, put it into commercial use in 1892. Acetylene, combined with oxygen, produces a flame temperature of 3100 °C, well above the melting point of most metals. With the development of torch systems in the late 1890s, the oxyacetylene welding and cutting processes were rapidly developed. John M. Morehead later became Vice-President of the American Welding Society (AWS) when it was founded in 1919 immediately after World War I, by members of the Wartime Welding Committee of the Emergency Fleet Corporation.

In 1856, James Joule, an Englishman, first experimented with welding a bundle of wire in charcoal by heating with an electric current. This technique of producing a weld by heating metal pieces by internal resistance was further developed to what now known as resistance welding by Elihu Thompson in 1885-1890. During the early 20th century, welding technology advanced quickly as World War I and World War II caused a major surge in the demand for reliable and inexpensive metal joining methods. Following the wars, several modern welding techniques

were developed, including shielded metal arc welding, gas metal arc welding, submerged arc welding, flux-cored arc welding and electroslag welding. Laser beam welding and electron beam welding were invented in the latter half of the century. Today, welding technology continues to advance, and new welding methods will be developed as greater understanding of weld quality and properties is gained (Wikimedia Foundation Inc., 2010).

## **Welding Processes**

As defined by AWS, welding is “a method for joining materials by fusing of the surfaces of two work pieces to form one”. The importance of welding in society is tremendous. No other technique is as widely used to join metals and alloys efficiently. Most of the familiar objects in modern society, from buildings and bridges, to vehicles, computers, and medical devices, could not be produced without the use of welding. Welding provides stronger joint for metal pieces than other joining techniques such as riveting and bolting. Welding is also stronger than other allied hot processes such as soldering and brazing, in which a lower-melting-point material is melted between the work pieces to form a bond without melting the work pieces. Wherever there are metals there is welding. AWS lists eighty welding processes in general industrial use. These processes can be classified into five categories: arc welding, gas welding, resistance welding, energy beam welding and solid-state welding. Energy beam welding includes laser beam welding, electron beam welding, and newly developed laser-hybrid welding and X-ray welding. Besides forge welding, common types of solid-state welding include ultrasonic welding, explosion welding, cold welding, diffusion welding, and high frequency welding, etc. Based on the widespread use and the potential for significant exposure to welders, arc welding, gas welding, and resistance welding are more of concern than energy beam welding and solid-state welding. Specific arc welding processes, as well as gas welding and resistance welding are briefly described below.

- Shielded metal arc welding (SMAW), also known as manual metal arc welding (MMA) or stick welding, is the most popular welding process all over the world, accounting for more than 50% of welding (Ulfvarson and Tech, 1981). The consumable electrode rod used in SMAW is made of flux-covered steel. The electrode core itself acts as filler material. Flux is a substance used in welding to facilitate the flow of molten metal and to protect the weld area from oxidation and contamination.
- Gas tungsten arc welding (GTAW), also known as tungsten inert gas (TIG) welding, uses a non-consumable tungsten electrode and a separate filler material. An inert or semi-inert gas mixture is used to protect the weld.
- Gas metal arc welding (GMAW), also known as metal inert gas (MIG) welding, uses a continuous wire feed as a consumable electrode and an inert or semi-inert gas mixture to protect the weld from contamination.
- Flux-cored arc welding (FCAW) uses a continuously-fed wire as consumable electrode, which consists of a steel electrode surrounding a powder flux/fill material. Although an externally supplied shielding gas is sometimes used, the flux itself is often relied upon to generate the necessary protection for the weld from the atmosphere. As the welding can be performed at high speed and the device is portable, the FCAW process is widely used in construction.

- Submerged arc welding (SAW) requires a continuously fed consumable electrode and a separate flux material. During welding, the arc is struck beneath a covering layer of granular fusible flux. The molten weld and the arc zone are completely covered by the thick layer of flux and thus protected from the atmospheric contamination. As the arc and the molten metal are covered, spatter and sparks are prevented and the intense ultraviolet radiation and fumes are suppressed as well.
- Plasma arc welding (PAW), advancement over the GTAW process, uses a non-consumable tungsten electrode and an arc constricted through a fine-bore copper nozzle. An inert or semi-inert gas mixture is used to protect the weld. The key difference from GTAW is that in PAW, by positioning the electrode within the body of the torch, the plasma arc can be separated from the shielding gas envelope. Therefore, temperature in PAW can approach 20,000 °C;
- Resistance welding uses the heat generated by passing current through the resistance caused by the contact between two metal surfaces to melt and thus joint metal pieces together. In general, resistance welding is efficient and causes little pollution. Resistance welding includes spot welding, seam welding, projection welding and flash butt welding, flash welding, and upset welding.
- Gas welding is one of the oldest and most versatile welding processes. All the gas welding methods are quite similar, generally differing only in the type of gases used. The most common one is oxyacetylene welding. Other methods include air acetylene welding, oxygen hydrogen welding, and pressure gas welding. Although due to its portability and relatively low cost gas welding was a popular welding method when it was first developed, it was largely replaced with arc welding in the 20th century as flux for the electrode continued to be developed (Wikimedia Foundation Inc., 2010).

## Health hazards in welding

During welding, welders are exposed to chemical, physical and radiation hazards. Chemical hazards include particulate matter containing metal constituents such as aluminum, cadmium, chromium, copper, iron, lead, manganese, magnesium, molybdenum, nickel, titanium and zinc; non-metal constituents such as fluorides and silica; and gases such as carbon monoxide and carbon dioxide, nitrogen monoxide (aka nitric oxide) and nitrogen dioxide, ozone, and decomposition of degreasing chemicals such as chlorinated hydrocarbons. Heat, vibration and noise are common physical agents to which welders are exposed. Welders are also exposed to ultraviolet, visible and infrared radiant energies. All these exposures are associated with potential adverse health effects. However, exposure to particulate matter and gases are considered more harmful in comparison with other exposures (Burgess, 1995; Antonini, 2003).

Human studies have indicated that exposure to welding fume causes, or potentially causes, respiratory effects including impaired lung function, metal fume fever, occupational asthma, bronchitis, pneumoconiosis and pulmonary fibrosis, respiratory infection and immunity deficiencies, and lung cancer. Welding fumes may also adversely affect dermal, cardiovascular, reproductive and neurological systems(ATSDR, 2008). Observed increased risks of lung cancer among welders are associated with exposure to nickel and hexavalent chromium in welding fume. Metal fume fever is typically caused by welding on galvanized steel that contains zinc. Long-term exposure to welding fumes leads to a pneumoconiosis referred to as siderosis. Potential neurological effects in welders are associated with exposure to airborne manganese (Antonini,

2003). The International Agency for Research on Cancer (IARC) classified welding fumes as a possible human carcinogen (Group 2B) because of apparent increased risks of lung cancer among welders (International Agency for Research on Cancer, 1990).

## **Manganese and welding**

Manganese naturally occurs in rocks, soil, water and food. It is an essential nutrient for humans. However, high level exposure causes adverse neurological, respiratory effects and probably hematological, endocrine and reproductive effects (ATSDR, 2008). Among these effects, neurological effects via inhalation are of most concern, as manganese primarily targets the central nervous system. The probable mechanism is that manganese enhances autoxidation, leading to increased production of free radicals, reactive oxygen species and other cytotoxic metabolites that may damage neurons(ATSDR, 2008). Although the precise biochemical mechanism remains unclear, studies of miners and factory workers provide clear evidence of neurological impairments induced by high level exposure to manganese via inhalation (Schuler, 1957; Mena et al., 1967; Smyth, 1973; ATSDR, 2008). The neurological syndrome is often referred to “Manganism”. Symptoms often start with subjective signs, such as weakness, anorexia, headache, lethargy, heaviness or stiffness of the legs and muscle pain. As the disease progresses, early clinical signs that may occur include altered gait, speech disturbance, emotionless facial expression and fine tremor. Severe Manganism patients may eventually become disabled from rigorous hypertonia and muscle rigidity (Schuler, 1957; Mena et al., 1967; Smyth, 1973; Saric, 1977; ATSDR, 2008).

Manganese is a common component in base metal and welding electrodes. It is used in steel alloys to improve metallurgical properties and provide both strength and hardness to the metal. Manganese is also an alloying element in non-consumable welding electrodes, as well as in consumables, with electrodes containing 0.4% to 15% of manganese. Manganese in welding material provides deoxidizing reactions and minimizes weld impurities (Santamaria et al., 2007). It is estimated that there are one million full-time and five million part-time welders worldwide. Given a variety of types of welding processes and their wide range of applications, welders are probably the largest occupation group exposed to airborne manganese. However, welders’ exposures to manganese and potential neurological effects have not been well-assessed. Studies evaluating welders’ neurological health status often provide very limited or no exposure data (Santamaria et al., 2007). The number of exposure studies is sparse and few of them assessed association between manganese exposure and process type, material composition, work load and ventilation. Although several epidemiological studies suggest that welders as a group have increased rates of neurological symptoms and lower scores on neurological function tests compared to control groups (Chandra et al., 1981; Sjogren et al., 1990; Sjogren et al., 1996; Bowler et al., 2003; Bowler et al., 2006; Park et al., 2006; Bowler et al., 2007), due to lack of sufficient exposure data and high quality exposure assessment, the causal relationship between exposure to airborne manganese and the adverse neurological effects in welders remains controversial.

Welding fumes are not currently regulated by the U.S. Occupational Safety and Health Administration (U.S. OSHA) permissible exposure level (PEL). The PEL for manganese compounds and manganese in fumes is  $5\text{mg}/\text{m}^3$ , expressed as the ceiling (OSAH, 1989), comparable to the current PEL for nuisance respirable particles that is also  $5\text{mg}/\text{m}^3$ , indicating that manganese toxicity is not appropriately considered. The American Conference of

Governmental Industrial Hygienists (ACGIH) Threshold Limit Value (TLV) is  $0.2\text{mg}/\text{m}^3$  for manganese in total dust, including elemental and inorganic compounds (ACGIH, 2010). A dose-response study using a benchmark dose model approach to analyze data from two previous studies resulted in 95% lower bound  $\text{BMD}_{10}$  for eight neurological endpoints ranging from  $0.09 - 0.27 \text{ mg Mn}/\text{m}^3$  in respirable dust, indicating that exposures below the current TLV may still pose risks for workers to develop subclinical neurological effects (Roels et al., 1992; Gibbs et al., 1999; Clewell et al., 2003). Based on the emerging evidence, ACGIH has proposed a TLV for manganese in respirable particles (separately from the current TLV for manganese in total particles) and the value has been proposed to be  $0.02\text{mg}/\text{m}^3$  (ACGIH, 2010).

## Work in this Dissertation

In order to better understand welders' exposures to particulate matter and manganese in welding fumes, three research projects were conducted. First, exposure data were compiled from multiple sources to elaborate a comprehensive picture of welding fume exposure. Two thousand and sixty five air measurements of total particulate matter and 697 measurements of manganese were analyzed using a combination of multivariable linear regression models and linear mixed models to identify important exposure determinants of welding fume exposures while simultaneously estimating variance components of the exposures between groups, between workers within groups, and within workers over time. The estimated fixed effects and variance components were used to compute the probabilities of exceeding particular occupational exposure limits. This study is described in Chapter Two of this dissertation.

After looking at exposures to total particulate and manganese in welding fumes in different industry over time, I examined the spatial distribution of welding fume exposure in an automobile assembly facility. A particle mapping study was conducted in this auto-assembly plant as a follow-up study to evaluate the effectiveness of ventilation improvement. The study explored how a mapping method could be dictated by study aims and process/facility characteristics, with an emphasis on evaluating and incorporating temporal variations in the process of analyzing spatial distributions; following a mapping protocol developed specifically for this work place, the study analyzed temporal and spatial variations in particle air concentrations, and identified high concentration areas that required further investigation and potentially higher level of controls; particle size distribution was also evaluated. Recommendations were made on developing controls with consideration of effects of particle size on exposures. Strategies for designing a mapping method are summarized. This work is reported in the Chapter Three of this dissertation.

In Chapters Two and Three, I found that exposures to particulate matter and manganese in welding fumes were greatly affected by potential exposure determinants such as process/work environment conditions. These exposure determinants are crucial not only to particulate and manganese air concentrations, but also to their size distributions, an exposure characteristic that fundamentally influences the toxicity of particles and manganese. In order to better understand welders' exposure to airborne manganese in welding fumes, a pilot study was conducted in three Chinese manufacturing facilities to characterize welders' exposure to airborne manganese from common welding processes, with emphasis on manganese distribution in submicrometer particles. The specific aims were to determine to what extent manganese in welding fumes was associated with fine and ultrafine particles; and to examine how manganese air concentration and size distribution were associated with welding process type, material, work load and work

environment. The welding processes investigated were shielded metal arc welding, gas metal arc welding, submerged arc welding and plasma arc welding. This study is reported in the Chapter Four of this dissertation.

## Reference

- ACGIH. (2010) TLVs and BEIs Based on the Documentation of the Threshold Limit Values for Chemical Substances and Physical Agents & Biological Exposure Indices. Cincinnati, Ohio: ACGIH.
- Antonini JM. (2003) Health effects of welding. *Critical Reviews in Toxicology* **33**: 61-103.
- ATSDR. (2008) Toxicological profile for manganese U.S. Department of Health and Human Services.
- Bowler RM, Gysens S, Diamond E, Booty A, Hartney C, Roels HA. (2003) Neuropsychological sequelae of exposure to welding fumes in a group of occupationally exposed men. *International Journal of Hygiene and Environmental Health* **206**: 517-529.
- Bowler RM, Gysens S, Diamond E, Nakagawa S, Drezgic M, Roels HA. (2006) Manganese exposure: Neuropsychological and neurological symptoms and effects in welders. *Neurotoxicology* **27**: 315-326.
- Bowler RM, Roels HA, Nakagawa S, Drezgic M, Diamond E, Park R, et al. (2007) Dose-effect relationships between manganese exposure and neurological, neuropsychological and pulmonary function in confined space bridge welders. *Occupational and Environmental Medicine* **64**: 167-177.
- Burgess WA. (1995) *Recognition of Health Hazards in Industry; A Review of Materials and Processes*. 2nd New York: John Wiley & Sons. ISBN 0 471 57716 2.
- Cary HB, Helzer SC. (2004) *Modern welding technology 6th*. Upper Saddle River, NJ: Prentice-Hall. ISBN 0 131 13029 3.
- Chandra SV, Shukla GS, Srivastava RS, Singh H, Gupta VP. (1981) An exploratory-study of manganese exposure to welders. *Clinical Toxicology* **18**: 407-416.
- Clewell HJ, Lawrence GA, Calne DB, Crump KS. (2003) Determination of an occupational exposure guideline for manganese using the benchmark method. *Risk Analysis* **23**: 1031-1046.
- Gibbs JP, Crump KS, Houck DP, Warren PA, Mosley WS. (1999) Focused medical surveillance: A search for subclinical movement disorders in a cohort of US workers exposed to low levels of manganese dust. *Neurotoxicology* **20**: 299-313.
- International Agency for Research on Cancer. (1990) *IARC Monograph on the evaluation of carcinogenic risks to humans Vol. 49: Chromium, Nickel and Welding*. Lyon: World Health Organization.
- Mena I, Marin O, Fuenzali S, Cotzias GC. (1967) CHRONIC MANGANESE POISONING - CLINICAL PICTURE AND MANGANESE TURNOVER. *Neurology* **17**: 128-&.
- OSAH (1989). *Rules and Regulations - CFR 1910 "Air Contaminants"*.
- Park RM, Bowler RM, Eggerth DE, Diamond E, Spencer KJ, Smith D, et al. (2006) Issues in neurological risk assessment for occupational exposures: The Bay Bridge welders. *Neurotoxicology* **27**: 373-384.
- Roels HA, Ghyselen P, Buchet JP, Ceulemans E, Lauwerys RR. (1992) Assessment of the Permissible Exposure Level to Manganese in Workers Exposed to Manganese-Dioxide Dust. *British Journal of Industrial Medicine* **49**: 25-34.
- Santamaria AB, Cushing CA, Antonini JM, Finley BL, Mowat FS. (2007) State-of-the-science review: Does manganese exposure during welding pose a neurological risk? *Journal of Toxicology and Environmental Health-Part B-Critical Reviews* **10**: 417-465.

- Sapp ME. A History of Welding: from Hepheastus to Apollo. December 18, 2009. Retrieved May 13, 2010, from <http://weldinghistory.org/whistoryfolder/welding/index.html>.
- Saric M, Markicevic, A., and Hrustic, O. (1977) Occupational exposure to manganese. *Br. J. Ind. Med.* **34**: 114-118.
- Schuler P, Oyanguren, H., Maturana, V., Valenzuela, A., Cruz, E., Plaza, V., Schmidt, E., and Haddad, R. (1957) Manganese poisoning: Environmental and medical study at a Chilean mine. *Industrial medicine and surgery* **26**: 167-173.
- Sjogren B, Gustavsson P, Hogstedt C. (1990) Neuropsychiatric symptoms among welders exposed to neurotoxic metals. *British Journal of Industrial Medicine* **47**: 704-707.
- Sjogren B, Iregren A, Frech W, Hagman M, Johansson L, Tesarz M, et al. (1996) Effects on the nervous system among welders exposed to aluminium and manganese. *Occupational and Environmental Medicine* **53**: 32-40.
- Smyth LT, Ruhf, R. C., Whiteman, N. E., and Dugan, T. . (1973) Clinical manganism and exposure to manganese in the production and processing of ferromanganese alloy. *Journal of Occupational Medicine* **15**: 101-109.
- Ulfvarson U, Tech D. (1981) Survey of air contaminants from welding. *Scandinavian Journal of Work Environment & Health* **7**: 1-28.
- Wikimedia Foundation Inc. Welding. June 3, 2010. Retrieved June 8, 2010, from <http://en.wikipedia.org/wiki/Welding>.

## Chapter 2:

# Application of Mixed Models to Assess Welding Exposures to Total Particulate Matter and Manganese

## Introduction

Welders are exposed to metal fumes, toxic gases, noise and ultraviolet and infrared radiations. Welding fumes cause respiratory damage, and may also adversely affect dermal, cardiovascular, reproductive and neurological systems (Antonini, 2003; Kim et al., 2005; Antonini et al., 2006; ATSDR, 2008). The International Agency for Research on Cancer (IARC) classified welding fumes as a possible human carcinogen (Group 2B) because of apparent increased risks of lung cancer among welders (International Agency for Research on Cancer, 1990). Because there are roughly 80 welding processes in general industrial use (Burgess, 1995), welders' exposures can potentially be influenced by the type and operation of the process, the composition of welded material and consumables, the work load, the ventilation conditions, etc. Although, many studies have been conducted to examine welding fume exposures and their determinants (Smith, 1967; Pantucek, 1971; Sanderson, 1972; Pantucek, 1975; Kobayashi et al., 1978; American Welding Society, 1979; Ulfvarson and Tech, 1981; Dryson and Rogers, 1991; Castner and Null, 1998; Pires et al., 2006; Flynn and Susi, 2010b), none have used sufficiently large datasets to examine exposures from different countries, industries, processes and jobs.

In order to elaborate a comprehensive picture of welding fume exposure, 2065 air measurements of total particulate matter (TP) and 697 measurements of manganese (Mn) were compiled from international sources. These data were analyzed using a combination of multivariable linear regression models and linear mixed models. Our goal was to identify important exposure determinants of welding fume exposures while simultaneously estimating variance components of the exposures between groups, between workers within groups, and within workers over time. Finally, the estimated fixed effects and variance components were used to compute the probabilities of exceeding particular occupational exposure limits (OELs).

## Methods

### *Data compilation*

The scientific literature, mainly in the fields of occupational hygiene and occupational epidemiology, was reviewed to retrieve exposure measurements during welding and allied hot processes (Steel and Sanderson, 1966; Sanderson, 1968; Tola et al., 1977; Goller, 1985; Dryson and Rogers, 1991; Fairfax, 1994; Barrington et al., 1998; Rappaport et al., 1999; Korczynski, 2000; Wallace et al., 2001; Wallace and Fischbach, 2002; Wurzelbacher et al., 2002). Publicly accessible governmental reports from the National Institute for Occupational Safety and Health (NIOSH) were obtained and exposure data were retrieved (NIOSH Health Hazard Evaluations, 1973-2000)<sup>1</sup>. A welding-fume database containing exposures in a variety of industrial sectors in

---

<sup>1</sup> Data were retrieved from following NIOSH reports: HETA 73-47-172, HETA 73-130-94, HETA 74-28-164, HETA 76-115-425, HETA 78-89-550, HETA 82-110-1288, HETA 85-030-1693, HETA 85-045-1762, HETA 85-

Europe and North America was also incorporated (TWI Welding fume exposure data, 2009). Since the TWI data included some NIOSH Health Hazard Evaluations, redundant data were removed. Besides welding, measurements from thermal cutting, arc gauging, brazing and burning were included when they were reported. The final data file included 28 sets of data, in which exposures were reported as individual measurements. Air concentrations of TP and Mn reported as lower than the limit of detection (LOD) were assigned a value of  $\text{LOD}/\sqrt{2}$  (Hornung and Reed, 1990). If the LOD was not reported, the lowest reported level from the same sampling site was used as a surrogate for the LOD. Along with the exposure measurements, the following details of the sampling regimen and exposure covariates were recorded: experimental vs. observational study, personal vs. area sample, sampling duration, country, industrial sector, type of welding process or hot work, base metal, and consumable used. Work practice and workplace environment were characterized as being either indoor or outdoor, confined space (enclosed space defined as less than  $27 \text{ m}^3$  or  $1000 \text{ ft}^3$ ) and according to the type of ventilation.

### ***Statistical modeling***

Separate statistical modeling was performed for TP and Mn measurements using the natural logarithm of the air concentration as the dependent variable. We adopted a two-step strategy for building models for these dependent variables. First, we screened all possible fixed effects using the following multivariate model:

$$Y_{h(kjl)} = \ln(X_{h(kjl)}) = \beta_0 + \sum_{u=1}^U \beta_u C_{u_{h(kjl)}} + e_{h(kjl)}, \quad (\text{Equation 1})$$

for  $h = 1, 2, \dots, H$  groups;

$k = 1, 2, \dots, K_h$  individual workers in the  $h$ -th group;

$j = 1, 2, \dots, J_{h(k)}$  sampling days of the  $k$ -th individual worker in the  $h$ -th group; and

$l = 1, 2, \dots, L_{h(kj)}$  measurements on the  $j$ -th sampling day of the  $k$ -th worker in the  $h$ -th group,

where,  $X_{h(kjl)}$  represents the  $l^{\text{th}}$  exposure measurement (TP or Mn) on the  $j$ -th sampling day of the  $k$ -th worker in the  $h$ -th group. (Because measurements reported in a given study were often collected from multiple worksites, data were grouped by sampling site).  $Y_{h(kjl)}$  is the natural logarithm of the individual measurement  $X_{h(kjl)}$ ;  $\beta_0$  is a intercept representing the true underlying global mean (logged) averaged over all covariate categories;  $\sum \beta_u C_{u_{h(kjl)}}$  represents the fixed effects from covariates  $C_1, C_2, \dots, C_U$ , and  $\beta_u$  is the regression coefficient of the  $u^{\text{th}}$  covariate. The exposure covariates were the variables related to processes, material, workplace environment characteristics, industry/trade, country, study type and sampling regimen (Table 1). The error term  $e_{h(kjl)}$  represents the random effect of the  $l$ -th measurement on the  $j$ -th day of the  $k$ -th individual worker in the  $h$ -th group. It is assumed that  $e_{h(kjl)}$  is normally distributed with means of zero and variances of  $\sigma^2_{Y,h}$  (representing the total variance of the logged exposure  $Y_{h(kjl)}$ ). Important covariates were screened using adjusted *P-Values* of the variables. First, each

---

046-1763, HETA 85-044-1761, HETA 85-252-1625, HETA 86-162-1782, HETA 86-524-1851, HETA-91-0142, HETA 93-0035-2481, HETA 93-0455-2342, HETA 94-0103-2440, HETA 94-0417-2505, HETA-97-0196-2755, HETA 97-0260-2716, HETA-99-0144-2797, HETA-2000-0185-2808, ECTB 214-11a, and ECTB 214-12a.

individual covariate was fitted into a regression model separately with all levels within the variable. “TEST” statement was used to obtain an un-adjusted *P-Value* for the covariate. Then, all covariates were fitted into a regression model with all levels within each variable. Separated “TEST” statements were used to obtain adjusted *P-Values* for the covariates. All the exposure covariates were ranked in the adjusted *P-Values*. The smaller the *P-Value*, the more important a covariate is to the exposure. Using  $P < 0.10$  as a criterion, covariates with *P-Values*  $< 0.05$  were selected to be fitted into mixed model.

After screening the fixed effects, selected covariates were fitted by mixed models defined by the following expression (Rappaport and Kupper, 2008):

$$Y_{h(kjl)} = \ln(X_{h(kjl)}) = \beta_0 + \sum_{u=1}^U \beta_u C_{u_{h(kjl)}} + b_h + d_{h(k)} + f_{h(kj)} + e_{h(kjl)}, \quad (\text{Equation 2})$$

where all common terms are the same as for Equation 1. The pre-screened exposure covariates were designated as fixed effects in the model while the variables *group*, *individual worker* and *sampling day* were designated as random effects. Therefore, the random effects were defined by a three-level nested structure, with variance components across groups, between workers (within groups) and within workers over time. In Equation 3,  $b_h$  represents the random effect of the  $h$ -th group;  $d_{h(k)}$  represents the random effect of the  $k$ -th individual worker in the  $h$ -th group;  $f_{h(kj)}$  represents the random effect of the  $j$ -th day of the  $k$ -th individual worker in the  $h$ -th group. It is assumed that  $b_h$ ,  $d_{h(k)}$ ,  $f_{h(kj)}$  and  $e_{h(kjl)}$  are normally distributed with means of zero and variances of  $\sigma_{bY,h}^2$ ,  $\sigma_{wY,h}^2$ ,  $\sigma_{wY,k}^2$  and  $\sigma_{wY,j}^2$  (representing the variance components between-group, within-group and between-worker, within-worker and between-day, and within-worker and within-day), and that the  $b_h$ ,  $d_{h(k)}$ ,  $f_{h(kj)}$  and  $e_{h(kjl)}$  are all statistically independent. Thus,  $\sigma_{Y,h}^2 = (\sigma_{bY,h}^2 + \sigma_{wY,h}^2 + \sigma_{wY,k}^2 + \sigma_{wY,j}^2)$  is the total variance of the logged exposure  $Y_{h(kjl)}$ . A compound symmetric variance-covariance structure was used.

We also used a random-effects model with the same three-level nested random effects as Model 3 to examine variance components without controlling for the fixed effects. The model is described as follows:

$$Y_{h(kjl)} = \ln(X_{h(kjl)}) = \beta_0 + b_h + d_{h(k)} + f_{h(kj)} + e_{h(kjl)}, \quad (\text{Equation 3})$$

where the random effects representing group, individual worker (within group) and day are defined as for the mixed model (Equation 2). The variance components estimated under Equations 2 and 3 were compared to assess the influence of fixed effects on the variance components. Data with missing information on exposure covariates were excluded from the models. All statistical analyses were performed using SAS software for Windows version 9.2 (SAS Institute Inc., Cary, NC, USA).

Finally, we computed two probabilities, namely the exceedance and the probability of overexposure, to assess relationships of TP and Mn exposures to particular occupational exposure limits (OELs) (TorneroVelez et al., 1997; Rappaport et al., 1999; Rappaport and Kupper, 2008). The exceedance ( $\gamma_h$ ), defined as the likelihood that a single daily air measurement for a randomly selected worker in the  $h$ -th group on a randomly selected day would exceed an OEL, is given by:

$$\gamma_h = P\{X_{h(ij)} > \text{OEL}\} = 1 - \Phi \left\{ \frac{\ln(\text{OEL}) - \mu_{Y,h}}{\sqrt{\sigma_{bY,h}^2 + \sigma_{wY,h}^2}} \right\}, \quad (\text{Equation 4})$$

where  $\Phi\{z\}$  denotes the probability that a standard normal variate would fall below the value  $z$  and  $\mu_{Y,h}$  is the mean (logged) exposure level for the  $h$ -th group. The probability of overexposure defines the likelihood that a randomly-selected worker's mean exposure in the  $h$ -th group (i.e.  $\mu_{X,h(i)}$ ) would be greater than an OEL and is given by:

$$\theta_h = P\{\mu_{X,h(i)} > OEL\} = 1 - \Phi\left\{\frac{\ln(OEL) - \mu_{Y,h} - \sigma_{wY,h}^2}{\sqrt{\sigma_{bY,h}^2}}\right\}. \quad (\text{Equation 5})$$

Estimates of the exceedance and probability of overexposure for the  $h$ -th group, designated  $\hat{\lambda}_h$  and  $\hat{\theta}_h$ , were obtained by substituting estimated parameters into Equations 4 and 5, respectively.

We estimated the exceedances and probabilities of overexposure for different countries and different industries based on the parameters estimated from the random effect model (Equation 3). As operative OELs, we used 5 mg/m<sup>3</sup> for TP, which had been the U.S. Occupational Safety and Health Administration (OSHA) Permissible Exposure Limit (PEL) until 1992 (Flynn and Susi, 2010a) and the American Conference of Governmental Industrial Hygienists (ACGIH) Threshold Limit Value (TLV) for total welding fumes prior to 2005, and 0.2 mg/m<sup>3</sup> for Mn, which has been the ACGIH TLV since 1992.

## Results

### *Descriptive analysis*

The final compiled dataset contained TP and Mn measurements collected in five countries (U.S., U.K., Canada, Finland and New Zealand), reflecting exposures in construction, shipbuilding, railroads, manufacturing and automobile industries from 1966 to 2005. The majority of the data were obtained by personal sampling in observational studies; a few data were collected as area samples (1.3% TP and 4.5% Mn) or from experimental studies of welding parameters (6.2% TP and 9.6% Mn). Specified welding processes included shielded-metal-arc welding, gas-metal-arc welding, gas-tungsten-arc welding, resistance welding and other (flux-cored-arc welding, submerged-arc welding and oxy-acetylene welding). The percentages of measurements below the LOD were 0.93% and 5.3% for TP and Mn, respectively. Repeated measurements accounted for 10% of TP and 19% of Mn measurements. Cumulative distribution plots for TP and Mn are presented in Figure 1. The overall arithmetic mean concentration (AM) was 4.79 mg/m<sup>3</sup> [standard deviation (SD) 11.8 mg/m<sup>3</sup>] and 0.502 mg/m<sup>3</sup> (SD 1.49 mg/m<sup>3</sup>) for TP and Mn, respectively. The geometric mean (GM) and geometric standard deviation (GSD) were 1.81 mg/m<sup>3</sup> and 4.04 for TP, and 0.160 mg/m<sup>3</sup> and 4.54 for Mn, respectively. Table 2 presents the summary statistics of TP and Mn data stratified by the exposure covariates. Although only very small portions of the data were from experimental studies or collected as area samples, these reported air concentrations were much higher than those from observational studies or personal samples. A sampling duration less than 60 minutes resulted in TP and Mn measurements 7-fold higher than when collected over longer time periods. Exposures in enclosed spaces or with only natural ventilation appeared much higher than those in open spaces or with mechanical or local-exhaust ventilation (LEV). Although Mn air concentrations were higher

indoors, TP concentrations showed no difference between indoors and outdoors, possibly because of the small number of outdoor measurements.

### ***Statistical modeling***

The un-adjusted and adjusted coefficient estimates for the covariates are presented in the Table 3 for TP and Table 4 for Mn. All the variables were significant by themselves. However, when other covariates were controlled, *consumable*, *type of work* and *indoor/outdoor* became insignificant to TP exposures, and *indoor/outdoor*, *duration*, *year*, *country* and *base metal* became insignificant to Mn exposures, using P-Value < 0.10 as a criterion. Due to a special interest at their effects on the exposures, *country* and *year* were still chosen to be fitted in the mixed model for Mn exposures. Therefore, mixed models for both TP and Mn had 11 covariates.

The fixed effects contained in the final mixed models for TP and Mn exposures are presented in Table 5 and Table 6, respectively, along with their coefficient estimates, 95% confidence intervals (CI), and the *P-Values* estimated by the mixed effect models (Equation 2). These fixed effects explained 55% and 49% of the total random variation in TP and Mn measurements, respectively, as estimated by the multivariate regression model (Equation 1). For TP, 20% and 18% of the total variation were explained by the sampling regimen and industry/trade, while 6% was explained by the process type and material, and exposure in the U.S. explained 8%. After controlling for other covariates, the mixed model showed that TP air concentrations measured in experimental studies or measured as area samples were significantly higher than those measured in observational studies or measured as personal samples. As indicated by the variable *year*, TP exposure showed no apparent changes over the examined time period (1966-2005). TP concentrations in the U.S. were significantly higher than they were in the U.K., but there were no differences between the U.K. and other tested countries. Significant effects of the degree of confinement and ventilation were observed, with TP concentration increasing 162% in enclosed spaces and decreasing 59% with the presence of LEV. Among four different trades, *welder fitters* had the lowest TP exposure and *boiler makers* had the highest TP exposure (significantly higher than for *welder fitters*). *Resistance welding* resulted in significantly lower exposure to TP. When welding was performed on *mild steel base metal*, TP concentrations were significantly higher compared to welding with *high alloy steel*.

For Mn measurements, 17% and 12% of the total variation were explained by the sampling regimen and ventilation, respectively. Industry/trade only explained 6% of the total variation, while the process type and material explained 9%. The variables for sampling regimen had no apparent effects on Mn exposures. Unlike for TP exposures, Mn exposures in the U.S. did not significantly differ from those in other countries. Parameter estimates for the variable *year* indicated no reductions in Mn exposures over the years for which measurements were available. *Industry* and *trade* appeared to have no significant effects on Mn exposure. Among *types of work* and *welding processes*, *thermal cutting* and *brazing* produced significantly higher Mn concentrations compared to *welding*, and *resistance welding* produced significantly lower exposures to Mn compared to *gas tungsten arc welding* (Table 6). As to the influence of materials used, *base metal* had no apparent effect on Mn exposure. Three out of seven consumables in the final model had significant effects and one had borderline significant effect. *Welding with no consumable* produced lower Mn exposures; welding with *flux cored*

*consumable, high-Mn-content consumable and gas-metal-arc welding with carbon-steel consumable* resulted in higher exposures.

Results from applications of the random-effects models (Equation 3) indicated that the between-group variance component ( $\sigma^2_{bY,h}$ ) produced the greatest percentages of variation for both TP and Mn exposures (53% for TP and 44% for Mn) and that the within-worker variance component reflecting day-to-day variation ( $\sigma^2_{wY,k}$ ), produced the smallest percentages for either contaminant (4 – 5%). The between-worker (within-group) variance components ( $\sigma^2_{wY,h}$ ) represented 23% and 16% of the total variability for TP and Mn, respectively (Table 7). The major difference in random effects models (Equation 3) of the two contaminants concerned the within-worker within-day variance component ( $\sigma^2_{wY,j}$ ), which represented a much larger percentage of the variance of Mn exposure than of TP exposure (36% vs. 19%). When the fixed effects were added, the mixed models (Equation 2) for TP and Mn exposures showed that the between-group variance component ( $\sigma^2_{bY,h}$ ) and within-group variance component ( $\sigma^2_{wY,h}$ ) were reduced substantially, both in absolute value and as percentages of total random variation. In contrast, addition of fixed effects had no discernable effect on the absolute magnitudes of the within-worker day-to-day variance component ( $\sigma^2_{wY,k}$ ) or the within-worker within-day variance component ( $\sigma^2_{wY,j}$ ). Consequently, under the mixed models, the within-worker variance components contributed proportionally more of the total random variation (i.e.,  $\sigma^2_{wY,k} + \sigma^2_{wY,j} = 60\%$  of  $\sigma^2_{Y,h}$  for TP and  $70\%$  of  $\sigma^2_{Y,h}$  for Mn) than under the random-effects model (i.e.,  $\sigma^2_{wY,k} + \sigma^2_{wY,j} = 24\%$  of  $\sigma^2_{Y,h}$  for TP and  $40\%$  of  $\sigma^2_{Y,h}$  for Mn).

The estimated exceedance ( $\hat{\lambda}_h$ ) and probability of overexposure ( $\hat{\theta}_h$ ) for group  $h$  are presented in Table 8 for the countries and industries with available data. Estimates of exceedances and probabilities of overexposure were unacceptably large ( $> 0.10$ ) for all countries, except for TP exposures in the U.K., and for all industries, except for TP exposures in the automobile assembly industry. Estimated probabilities were much greater for Mn (OEL =  $0.2 \text{ mg/m}^3$ ) than for TP exposures (OEL =  $5 \text{ mg/m}^3$ ). Exposure to Mn in the U.S. had the highest estimated exceedance (35%) and probability of overexposure (51%) of all countries evaluated. Also, the highest probabilities for Mn exposure were observed in the railroad industry, where estimates of the exceedance and the probability of overexposure were 66% and 87%, respectively.

## Discussion

### *Exposure determinants*

When fixed effects were added to mixed models of exposure to TP and Mn, the total random variation ( $\sigma^2_{Y,h}$ , as indicated by the sum of all variance components) was reduced dramatically, i.e., from 2.12 to 0.88 for TP and from 3.91 to 2.19 for Mn (Table 7). This indicates that the mixed models identified important exposure determinants for TP and Mn in welding fumes. Air levels of both contaminants were much higher in enclosed spaces and were much lower when LEV was present (Tables 5 and Table 6). A recent study using several large data sets (including subsets of data used in this study) found that LEV could reduce welding fume exposures and that higher exposures were associated with a greater degree of confinement (Flynn and Susi, 2010b), consistent with findings of this study. The welding material also had

major effects on exposures. Exposure to TP increased when welding was performed on mild steel (Table 5). Regarding Mn exposure, most examined consumables significantly affected air levels, with high-Mn-content consumables profoundly increasing air levels of Mn (Table 6). The effect of high Mn content on exposure is also indicated by high Mn concentrations observed in the railroad industry, where steel often has a high Mn content. Among welding processes tested in this study, only *resistance welding* significantly affected exposures to TP and Mn, in both cases leading to lower air concentrations. Although some welding processes are thought to have higher fume generation rates than others (American Welding Society, 1979; Burgess, 1995), our results suggest that, in practice, exposures are largely driven by non-welding-process factors, such as work-space confinement, ventilation, workload, material used, etc. The variables *industry* and *trade* affected exposure to TP (higher in manufacturing and among boiler makers) and explained 18% of the total random variation in TP exposures but only 6% of variation in Mn exposures.

### ***Exposure levels***

Symanski et al. (1998) investigated long-term exposures to a wide range of airborne contaminants and found clear downward trends in exposures across industries worldwide from 1967 to 1996. They reported that 78% of 694 data sets showed linear trends towards lower exposure levels at a median rate of 8% per year (interquartile range: 4% - 14%). In contrast, our study found no reductions in TP and Mn exposures in welding fumes during the time period covered by the compiled data (1966 to 2005).

Moreover, the estimated exceedances and probabilities of overexposure indicated that air concentrations of TP and Mn were unacceptably high, using  $5 \text{ mg/m}^3$  and  $0.2 \text{ mg/m}^3$  as reference OELs for TP and Mn, respectively (Table 8). Indeed, the only estimated exceedances and probabilities of overexposure found to be less than 10% were for TP exposures in the U.K. and the automobile industry. The estimated exceedances and probabilities of overexposure were uniformly high (and unacceptable) for all factors affecting exposures to Mn (no Mn data were available from Finland and New Zealand). In most cases, the probability of overexposure was greater than the corresponding exceedance, which is consistent with earlier findings that when the exceedance is large (greater than about 0.20), the probability of overexposure tends to be even larger (Tornerovelez et al., 1997; Rappaport and Kupper, 2008). The high probabilities of exceedance estimated in this study are consistent with the findings of Flynn and Susi (2010b) who reported that Mn exposure from welding fumes were frequently at or above the TLV (note that some data sources overlapped with the current study).

The high and generally unacceptable levels of exposure to TP and Mn observed in our study are particularly troubling when considering that welding fumes are known to be harmful to human health. Welding fumes have been classified as a possible human carcinogen by IARC (Group 2B) and a potential occupational carcinogen for lung cancer by the National Institute for Occupational Safety and Health (NIOSH) (NIOSH, 2009). Thus, it is surprising that welding fumes are no longer covered by either an OSHA PEL (since 1992) or an ACGIH TLV (since 2005). OSHA expressed its intention to regulate individual constituents of welding fumes and thus more effectively control welding fume exposure. The ACGIH provided notice that it intends to lower the Mn TLV from  $0.2$  to  $0.02 \text{ mg/m}^3$  based on evidence that welders exposed to high levels of Mn experienced neurological effects (ACGIH, 2010). If a new TLV of  $0.02 \text{ mg/m}^3$

were to take effect, our results suggest that it would be exceeded in virtually all welding operations, with exceedances ranging from 56% to 96% and probabilities of overexposure ranging from 79% to 100%.

The high levels of exposure to welding fumes observed in our study are even more troubling in light of the fact that we detected no trend towards reduction in exposures to TP and Mn in welding operations over the past 40 years. This finding runs counter to the consistent reductions in air levels of most chemical agents (median reduction = 8%/year) that have been well documented over a similar time period (Symanski et al., 1998). Although one can only speculate about the utter failure to reduce exposures to such well known health hazards during the last half of the 20<sup>th</sup> century, it should be clear that something must be done to improve the situation.

### ***Controlling exposures to welding fumes***

The mixed models developed in this study identified some important determinants of exposures to TP and Mn, particularly the degree of confinement and LEV (Tables 5 and 6). This suggests that particular attention should be paid to controlling exposures in enclosed spaces and implementing improved ventilation practices in welding operations. Other important exposure determinants were different for TP and Mn exposures. The base metal was an important predictor of TP exposure while consumables were more important to Mn exposure. The variables *industry* and *trade* explained 18% of the total random variation in TP exposure (higher in manufacturing and among boiler makers). However, Mn exposure was affected less by *industry* and *trade*, which collectively explained only 6% of the variation. These findings indicate that, while focusing upon confined spaces and ventilation will affect both types of exposures, different control strategies may be needed to address particular sources of TP and Mn exposures. Thus, control strategies that target the industry and type of welding process, as typically used for controlling TP exposures, may not be appropriate for Mn exposures. Rather, the type and composition of welding consumables should be a major target for controls for Mn exposures. Moreover, we observed that within-worker variation in Mn exposure was three times larger than that in TP exposure, indicating great variability in Mn exposure from day to day and within a day for a given welder. While between-worker variability calls for individual-level controls to reduce exposure levels for highly exposed workers (investigating personal environments including location, types of equipment, and individual work practice), within-worker variability is more likely to result from environmental variables, including shared tasks, that affect all welders and thus require administrative and engineering solutions (Rappaport and Kupper, 2008).

## References

- ACGIH. (2010) TLVs and BEIs Based on the Documentation of the Threshold Limit Values for Chemical Substances and Physical Agents & Biological Exposure Indices. Cincinnati, Ohio: ACGIH.
- American Welding Society. (1979) Fume and Gases in the Welding Environment - A Research Report on Fumes and Gases Generated During Welding Operations Miami, Florida: American Welding Society.
- Antonini JM. (2003) Health effects of welding. *Critical Reviews in Toxicology* **33**: 61-103.
- Antonini JM, Santaimaria AB, Jenkins NT, Albini E, Lucchini R. (2006) Fate of manganese associated with the inhalation of welding fumes: Potential neurological effects. *Neurotoxicology* **27**: 304-310.
- ATSDR. (2008) Toxicological profile for manganese U.S. Department of Health and Human Services.
- Barrington WW, Angle CR, Willcockson NK, Padula MA, Korn T. (1998) Autonomic function in manganese alloy workers. *Environmental Research* **78**: 50-58.
- Burgess WA. (1995) Recognition of Health Hazards in Industry; A Review of Materials and Processes. 2nd New York: John Wiley & Sons. ISBN 0 471 57716 2.
- Castner HR, Null CL. (1998) Chromium, nickel and manganese in shipyard welding fumes. *Welding Journal* **77**: 223S-231S.
- Dryson EW, Rogers DA. (1991) Exposure to fumes in typical New-Zealand welding operations. *New Zealand Medical Journal* **104**: 365-367.
- Fairfax RE. (1994) Manganese exposure during welding operations. *Applied Occupational and Environmental Hygiene* **9**: 537-538.
- Flynn MR, Susi P. (2010a) Modeling mixed exposures: an application to welding fumes in the construction trades. *Stochastic Environmental Research and Risk Assessment* **24**: 377-388.
- Flynn MR, Susi P. (2010b) Manganese, Iron, and Total Particulate Exposures to Welders. *Journal of Occupational and Environmental Hygiene* **7**: 115-126.
- Goller JW, Paik, N. W. (1985) A comparison of iron-oxide fume inside and outside of welding helmets. *American Industrial Hygiene Association Journal* **46**: 89-93.
- Hornung RW, Reed LD. (1990) Estimation of average concentration in the presence of nondetectable values. *Applied Occupational and Environmental Hygiene* **5**: 132-141.
- International Agency for Research on Cancer. (1990) IARC Monograph on the evaluation of carcinogenic risks to humans Vol. 49: Chromium, Nickel and Welding. Lyon: World Health Organization.
- Kim JY, Chen JC, Kim JY, Christiani DC. (2005) Exposure to welding fumes is associated with acute systemic inflammatory responses. *Occupational and Environmental Medicine* **62**: 157-163.
- Kobayashi H, Nakamura Y, Ishiyama K. (1978) Measurements of fume produced during CO<sub>2</sub> gas welding *Journal of Mechanical Engineering Laboratory* **32**: 192-201.
- Korczyński RE. (2000) Occupational health concerns in the welding industry. *Applied Occupational and Environmental Hygiene* **15**: 936-945.
- NIOSH. Pocket Guide to Chemical Hazards: Welding Fumes. Retrieved May 10, 2010, from <http://www.cdc.gov/niosh/npg/npgd0666.html>
- NIOSH Health Hazard Evaluations. <http://www.cdc.gov/niosh/hhe/default.html> (Accessed June 9, 2006).
- Pantucek MB. (1971) Influence of filler materials on air contamination in manual electric arc welding. *American Industrial Hygiene Association Journal* **32**: 687-695.
- Pantucek MB. (1975) Hygiene evaluation of exposure to fluoride fume from basic arc welding electrodes. *Annals of Occupational Hygiene* **18**: 207-212.
- Pires I, Quintino L, Miranda RM, Gomes JFP. (2006) Fume emissions during gas metal arc welding. *Toxicological and Environmental Chemistry* **88**: 385-394.

- Rappaport SM, Weaver M, Taylor D, Kupper L, Susi P. (1999) Application of mixed models to assess exposures monitored by construction workers during hot processes. *Annals of Occupational Hygiene* **43**: 457-469.
- Rappaport SM, Kupper LL. (2008) *Quantitative Exposure Assessment*. El Cerrito, CA: Stephen Rappaport. 978-0-9802428-0-5.
- Sanderson JT. (1968) Hazards of the arc-air gouging process. *Ann Occup Hyg* **11**: 123-133.
- Sanderson JT. (1972) Exposure to manganese fume during welding with coated electrodes. *American Industrial Hygiene Association Journal* **33**: 13-18.
- Smith LK. (1967) Fume exposure from welding with low hydrogen electrodes. *Ann Occup Hyg* **10**: 113-121.
- Steel J, Sanderson JT. (1966) Toxic constituents of welding fumes. *Ann Occup Hyg* **9**: 103-111.
- Symanski E, Kupper LL, Rappaport SM. (1998) Comprehensive evaluation of long term trends in occupational exposure: part 1. Description of the database. *Occupational and Environmental Medicine* **55**: 300-309.
- Tola S, Kilpio J, Virtamo M, Haapa K. (1977) Urinary chromium as an indicator of exposure of welders to chromium. *Scandinavian Journal of Work Environment & Health* **3**: 192-202.
- TorneroVelez R, Symanski E, Kromhout H, Yu RC, Rappaport SM. (1997) Compliance versus risk in assessing occupational exposures. *Risk Analysis* **17**: 279-292.
- TWI Welding fume exposure data (2009). [http://www.twi.co.uk/content/fume\\_exposure\\_intro.html](http://www.twi.co.uk/content/fume_exposure_intro.html) (Accessed June 9, 2009).
- Ulfvarson U, Tech D. (1981) Survey of air contaminants from welding. *Scandinavian Journal of Work Environment & Health* **7**: 1-28.
- Wallace M, Shulman S, Sheehy J. (2001) Comparing exposure levels by type of welding operation and evaluating the effectiveness of fume extraction guns. *Applied Occupational and Environmental Hygiene* **16**: 771-779.
- Wallace M, Fischbach T. (2002) Effectiveness of local exhaust for reducing welding fume exposure during boiler rehabilitation. *Applied Occupational and Environmental Hygiene* **17**: 145-151.
- Wurzelbacher SJ, Hudock SD, Johnston OE, Blade LM, Shulman SA. (2002) A pilot study on the effects of two ventilation methods on weld fume exposures in a shipyard confined space welding task. *Applied Occupational and Environmental Hygiene* **17**: 735-740.

Figure 1 Cumulative distributions for air concentrations of total particulate matter (TP) and manganese (Mn) during welding and other hot processes. (The total numbers of measurements were 2065 for TP and 697 for Mn).

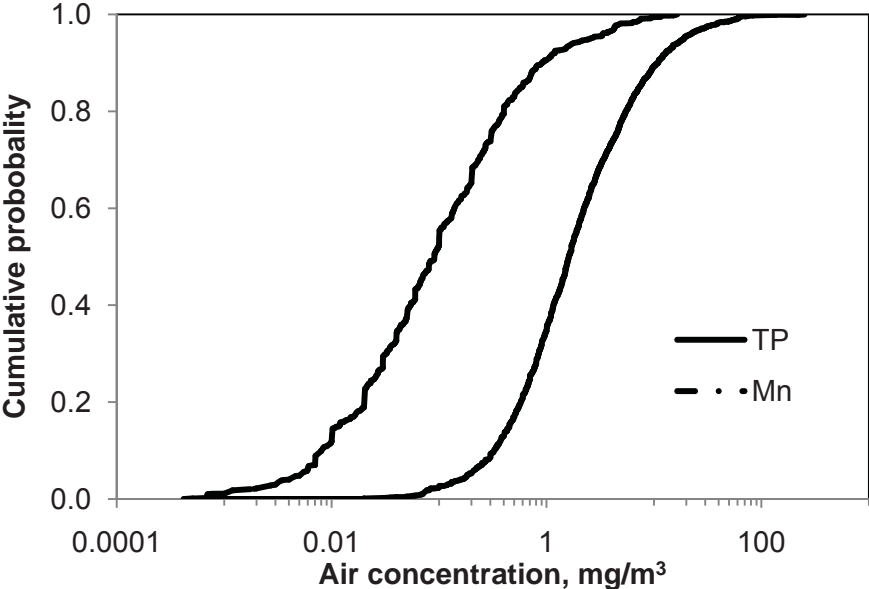


Table 1. Exposure covariates examined in the study.

Variable	Type	Values
Study type	Dichotomous	0: Observational 1: Experimental
Air sampling	Dichotomous	0: Personal 1: Area
Sampling duration	Dichotomous	0: Sampling duration $\geq$ 60 minutes 1: Sampling duration $<$ 60 minutes
Year	Continuous	1966 - 2005
Country	Nominal	0: Canada 1: Finland 2: New Zealand 3: U. K. 4: U. S.
Industry	Nominal	0: Construction 1: Manufacturing 2: Shipyard 3: Railroad 4: Automobile
Trade	Nominal	0: Boiler maker 1: Iron worker 2: Pipe fitter 3: Welder fitter
Type of Work	Nominal	1: Welding 2: Burning 3: Brazing 4: Arc gouging
Ventilation	Nominal	0: Natural 1: Mechanical 2: Local exhaust
Confined Space	Dichotomous	0: Open space 1: Enclosed space ( $<$ 27 m <sup>3</sup> or 1000 ft <sup>3</sup> )
Indoor/Outdoor	Dichotomous	0: Outdoor work 1: Indoor work
Welding Process	Nominal	0: Other (flux cored, submerged, oxy acetylene welding) 1: Shielded metal arc welding 2: Gas metal arc welding 3: Gas tungsten arc welding 4: Resistance welding
Base Metal	Nominal	0: Carbon steel 1: Mild steel 2: High alloy steel 3: Aluminum

Consumable

Nominal

- 4: Other
  - 0: Shield metal arc - carbon low alloy
  - 1: Shield metal arc - stainless steel high alloy
  - 2: Flux cored arc welding
  - 3: Gas metal arc - carbon steel
  - 4: Gas metal arc - stainless steel high alloy
  - 5: Gas metal arc - Al or Cu
  - 6: High manganese
  - 7: Submerged arc welding
  - 8: Welding with no consumables
  - 9: Other
-

Table 2. Summary statistics for exposures to total particulate matter (TP) and manganese (Mn) stratified by exposure covariates, mg/m<sup>3</sup>.

		Total particulate matter			Manganese		
		<i>n</i>	AM	SD	<i>n</i>	AM	SD
Study type	Observational	1945	3.76	7.43	636	0.347	0.977
	Experimental	120	21.5	34.6	61	2.12	3.59
Air sampling	Personal	2038	4.26	9.69	667	0.388	1.19
	Area	27	45.0	43.7	30	3.03	3.76
Sampling duration	< 60 minutes	121	26.4	36.4	72	2.33	3.42
	>= 60 minutes	1670	3.60	6.07	483	0.298	0.913
	Not specified	274	2.49	4.15	142	0.272	0.625
Country	Canada	73	2.76	3.40	115	0.236	0.556
	Finland	27	8.01	6.12	0	–	–
	New Zealand	18	2.32	2.36	0	–	–
	UK	1204	2.41	8.54	100	0.763	2.33
	US	743	8.78	15.4	482	0.511	1.42
Industry	Construction	277	5.49	6.40	198	0.132	0.233
	Manufacturing	109	10.5	7.42	21	0.476	0.967
	Shipyards	490	3.99	10.3	28	0.839	1.16
	Railroad	3	7.53	6.60	21	1.42	2.02
	Automobile	642	1.19	1.24	66	0.0931	0.131
	Not specified	544	8.24	16.6	363	0.701	1.77
Trade	Boiler maker	51	12.4	8.89	48	0.291	0.392
	Iron worker	57	7.07	6.51	13	0.126	0.0685
	Pipe fitter	80	3.21	3.26	47	0.0928	0.145
	Welder fitter	1875	4.58	12.1	588	0.561	1.62
Ventilation	Natural	792	6.60	16.0	256	0.800	2.17
	Mechanical	730	3.04	7.57	161	0.247	0.503
	Local exhaust	406	3.58	7.34	147	0.410	1.29
	Not specified	137	7.24	9.88	133	0.340	0.509
Degree of confinement	Open space	1370	3.51	6.76	462	0.270	0.663
	Enclosed space	387	8.15	18.7	53	2.17	3.15
	Not specified	308	6.23	16.2	182	0.604	1.91
Indoor/outdoor	Outdoor work	93	4.51	3.82	97	0.291	1.03
	Indoor work	1754	4.50	10.9	430	0.591	1.56
	Not specified	218	7.21	18.7	170	0.398	1.53
Continuous/intermittent	> 50% hot work	233	15.5	23.7	182	0.756	1.87
	<= 50% hot work	166	5.56	5.96	79	0.0644	0.0648
	Not specified	1666	3.21	8.40	436	0.475	1.44
Type of work	Thermal cutting	39	5.18	8.14	17	0.112	0.179
	Welding	1807	4.57	10.7	548	0.521	1.45
	Burning	5	3.85	4.73	9	0.0334	0.0309
	Brazing	26	2.81	2.46	12	0.0844	0.155

	Arc gouging	57	5.36	6.53	19	0.449	0.745
	Not specified	131	7.89	23.7	92	0.571	2.06
Welding process	Shielded metal arc	707	7.41	14.9	339	0.543	1.53
	Gas metal arc	388	5.48	9.19	232	0.360	0.899
	Gas tungsten arc	109	1.04	2.14	12	0.0408	0.0389
	Resistance welding	559	1.04	1.04	4	0.128	0.0126
	Other welding	42	2.00	2.09	17	1.66	3.20
	Allied hot process	97	4.63	5.85	23	0.0901	0.140
	Non-specified	163	1.60	1.47	70	0.732	2.34
Base metal	Carbon steel	173	5.43	5.50	171	0.213	0.536
	Mild steel	1367	4.99	11.7	411	0.610	1.61
	High alloy steel	317	4.92	16.4	88	0.640	2.17
	Aluminum	62	2.71	3.87	10	0.124	0.217
	Not specified	146	2.32	3.93	17	0.309	0.460
Consumable	Shielded metal arc welding - carbon low alloy	544	5.76	10.2	243	0.249	0.694
	Shielded metal arc welding - stainless steel	129	11.8	25.5	23	2.75	4.30
	Flux cored consumable	96	17.5	16.8	45	0.906	1.40
	Gas metal arc welding - carbon steel	200	3.71	3.92	157	0.423	1.36
	Gas metal arc welding - stainless steel	78	0.89	1.05	37	0.506	1.21
	Gas metal arc welding - Al or Cu	79	3.83	6.02	46	0.208	0.519
	High manganese consumable	5	11.0	4.77	5	2.84	1.21
	Submerged arc welding consumable	22	1.55	1.08	0	–	–
	No consumable	725	1.85	9.74	28	1.18	3.56
	Not specified	187	5.43	8.72	113	0.384	0.726

Legend: *n*, samples size; AM, arithmetic mean of measurements; SD, standard deviation.

Table 3 Results of un-adjusted and adjusted models for TP exposures

<u>Variable</u>	<u>Coefficient Estimate</u>	
	<u>Un-Adjusted</u>	<u>Adjusted</u>
Confined space		
Open space	Ref.	-
Enclosed space	0.440	0.480
Ventilation		
Natural	Ref.	-
Mechanical	-0.639	-0.085
Local exhaust	-0.309	-0.630
Country		
U.K.	Ref.	-
Canada	0.431	0
Finland	1.88	0
New Zealand	0.063	0.299
US	1.34	0.820
Trade		
Welder fitter	Ref.	-
Boiler maker	1.86	1.46
Iron worker	1.18	0.369
Pipe fitter	0.401	0.288
Other	-0.749	-1.34
Base metal		
High alloy steel	Ref.	-
Mild steal	0.376	0.883
Carbon steal	1.050	0.164
Aluminum	0.067	0.128
Other	-0.370	0
Industry		
Automobile assembly	Ref.	-
Construction	1.44	-0.023
Manufacturing	1.96	1.21
Railroad	0	0
Shipyard	0.481	0.474
None-specific	1.34	-0.032
Study type		
Observational study	Ref.	-
Experimental study	1.95	0.791
Sample type		
Personal sample	Ref.	-
Area sample	3.00	1.34

Duration		
Duration >= 60 minutes	Ref.	-
Duration < 60 minutes	2.00	0.621
Welding process		
Gas tungsten arc	Ref.	-
Shield metal arc	0.682	0.402
Gas metal arc	0.174	0.083
Other welding	-0.278	-0.706
None-welding	0.461	0.126
None-specific welding	-0.438	0.145
Resistance welding	-0.771	-0.596
Year		
(1 year change)	-0.058	0.021
Consumable		
SMAC-CLA	Ref.	
SMAC-SSHA	0.341	
Consumable-Flux Core	1.33	
GMAS-Al or Cu	-0.414	
GMAS-CS	-0.306	
GMAS-SSHA	-2.00	
High Manganese	1.33	
Consumable-None	-1.20	
Submerged Arc	-0.881	
Type of work		
Welding	Ref.	
Thermal cutting	0.215	
Burning	0.263	
Brazing	0.212	
Arc gouging	0.576	
Indoor/Outdoor		
Outdoor work	Ref.	
Indoor work	-0.706	

---

Table 4 Results of un-adjusted and adjusted models for Mn exposures

<u>Variable</u>	<u>Coefficient Estimate</u>	
	<u>Un-Adjusted</u>	<u>Adjusted</u>
Confined space		
Open space	Ref.	-
Enclosed space	2.369	1.528
Consumable		
SMAC-CLA	Ref.	-
SMAC-SSHA	1.858	0.554
Consumable-Flux Core	1.426	1.025
GMAS-Al or Cu	-0.730	-1.192
GMAS-CS	0.034	0.994
GMAS-SSHA	-0.328	0.664
High Manganese	3.508	1.759
Consumable-None	-0.303	-1.518
Submerged Arc	0	0
Type of work		
Welding	Ref.	-
Thermal cutting	-0.641	1.900
Burning	-1.874	-1.039
Brazing	-1.062	3.630
Arc gouging	0.746	2.630
Welding process		
Gas tungsten arc	Ref.	-
Shield metal arc	0.633	1.008
Gas metal arc	0.378	0.513
Other welding	0.169	0.784
None-welding	-0.367	-1.826
None-specific welding	0	0
Resistance welding	0.799	3.795
Trade		
Welder fitter	Ref.	-
Boiler maker	0.219	0.698
Iron worker	0.126	1.737
Pipe fitter	-0.891	-0.115
Other	-1.525	-1.551
Ventilation		
Natural	Ref.	-
Mechanical	-0.326	0.106
Local exhaust	-0.704	-0.898
Sample type		

Personal sample	Ref.	-
Area sample	2.723	1.755
Industry		
Automobile assembly	Ref.	-
Construction	0.725	-1.073
Manufacturing	1.125	0.000
Railroad	2.001	0.953
Shipyards	2.149	0.932
None-specific	1.573	0.164
Study type		
Observational study	Ref.	-
Experimental study	1.622	-1.244
Year		
(1 year change)	-0.056	-0.022
Country		
U.K.	Ref.	-
Canada	0.091	0
Finland	0	0
New Zealand	0	0
US	0.378	0.710
Indoor/Outdoor		
Outdoor work	Ref.	
Indoor work	0.682	
Duration		
Duration >= 60 minutes	Ref.	
Duration < 60 minutes	1.727	
Base metal		
High alloy steel	Ref.	
Mild steel	0.610	
Carbon steel	-0.032	
Aluminum	-0.412	
Other	0	

---

Table 5 Estimated coefficients, 95% CI and *P-Values* for TP exposures

<u>Variable</u>	<u>Estimate</u>	<u>95% CI</u>		<u>P-Value</u>
Study type				
Observational study	Ref.	---		---
Experimental study	1.34	0.625	- 2.06	0.0003
Sample type				
Personal sample	Ref.	---		---
Area sample	1.29	0.139	- 2.44	0.030
Duration				
Duration >= 60 minutes	Ref.	---		---
Duration < 60 minutes	0.199	-0.192	- 0.591	0.320
Year				
(1 year change)	-0.010	-0.039	- 0.018	0.485
Confined space				
Open space	Ref.	---		---
Enclosed space	0.494	0.313	- 0.676	<.0001
Ventilation				
Natural	Ref.	---		---
Mechanical	-0.063	-0.204	- 0.079	0.386
Local exhaust	-0.536	-0.737	- -0.336	<.0001
Country				
U.K.	Ref.	---		---
Canada	0	---		---
US	1.18	0.638	- 1.716	<.0001
Industry				
Automobile assembly	Ref.	---		---
Construction	-0.564	-1.48	- 0.348	0.228
Manufacturing	0.963	-0.024	- 1.95	0.058
Railroad	0	---		---
Shipyards	0.554	-0.249	- 1.36	0.178
None-specific	-0.506	-1.27	- 0.260	0.197
Trade				
Welder fitter	Ref.	---		---
Boiler maker	1.46	0.662	- 2.26	0.001
Iron worker	0.596	-0.279	- 1.47	0.184
Pipe fitter	0.065	-0.567	- 0.696	0.841
Other	-0.905	-2.68	- 0.875	0.320
Welding process				
Gas tungsten arc welding	Ref.	---		---
Shield metal arc welding	0.236	-0.033	- 0.506	0.088
Gas metal arc welding	0.032	-0.326	- 0.390	0.861

Other welding	-0.194	-0.603	-	0.215	0.353
None-welding	0.495	0.147	-	0.844	0.006
None-specific welding	0.220	-0.248	-	0.689	0.358
Resistance welding	-0.672	-1.09	-	-0.255	0.002
Base metal					
High alloy steel	Ref.		---		---
Mild steal	0.706	0.474	-	0.938	<.0001
Carbon steel	0.212	-0.294	-	0.717	0.413
Aluminum	0.325	-0.140	-	0.790	0.173

---

Table 6 Estimated coefficients, 95% CI and *P-Values* for Mn exposures

<u>Variable</u>	<u>Estimate</u>	<u>95% CI</u>		<u>P-Value</u>
Study type				
Observational study	Ref.	---		---
Experimental study	-0.748	-2.48	- 0.980	0.398
Sample type				
Personal sample	Ref.			
Area sample	1.32	-0.246	- 2.88	0.102
Year				
(1 year change)	-0.029	-0.095	- 0.037	0.395
Confined space				
Open space	Ref.	---		---
Enclosed space	1.43	0.699	- 2.16	0.0002
Ventilation				
Natural	Ref.	---		---
Mechanical	-0.020	-0.401	- 0.362	0.919
Local exhaust	-1.10	-1.70	- -0.512	0.000
Country				
U.K.	Ref.	---		---
Canada	2.43	-0.261	- 5.12	0.257
US	0.806	-1.52	- 3.13	0.498
Industry				
Automobile assembly	Ref.	---		---
Construction	-0.233	-3.14	- 2.68	0.876
Manufacturing	0.283	-3.19	- 3.75	0.873
Railroad	2.76	-0.951	- 6.47	0.148
Shipyard	1.51	-0.823	- 3.85	0.207
None-specific	0.168	-2.65	- 2.98	0.907
Trade				
Welder fitter	Ref.	---		---
Boiler maker	0.363	-1.44	- 2.17	0.694
Iron worker	0.511	-1.88	- 2.91	0.677
Pipe fitter	-0.788	-2.30	- 0.728	0.311
Other	-1.44	-4.08	- 1.20	0.288
Type of work				
Welding	Ref.	---		---
Thermal cutting	1.36	0.222	- 2.51	0.021
Burning	-0.948	-2.17	- 0.276	0.132
Brazing	2.82	0.641	- 5.00	0.013
Arc gouging	1.19	-2.60	- 4.97	0.541
Welding process				

Gas tungsten arc welding	Ref.		---		---
Shield metal arc welding	1.02	-0.055	-	2.10	0.066
Gas metal arc welding	0.453	-0.796	-	1.70	0.478
Other welding	0.314	-0.864	-	1.49	0.603
None-welding	-0.788	-3.62	-	2.05	0.587
None-specific welding	0		---		---
Resistance welding	-3.91	-6.85	-	-0.96543	0.011
Consumable					
SMAC-CLA	Ref.		---		---
SMAC-SSHA	0.330	-0.697	-	1.36	0.531
Consumable-Flux Core	2.37	1.44	-	3.31	<.0001
GMAS-Al or Cu	-0.441	-1.28	-	0.398	0.305
GMAS-CS	1.02	-0.083	-	2.13	0.073
GMAS-SSHA	-0.690	-2.03	-	0.645	0.313
High Manganese	2.13	0.906	-	3.35	0.001
Consumable-None	-1.44	-3.00	-	0.117	0.073
Submerged Arc	0		---		---

---

Table 7. Variance component estimates for the one-way random-effects (Equation 4) and mixed-effects models (Equation 3) for TP and Mn exposures.

Variance component	TP exposure		Mn exposure	
	Random effects model (Equation 3)	Mixed-effects model (Equation 2)	Random effects model (Equation 3)	Mixed-effects model (Equation 2)
$\sigma^2_{bY,h}$	1.124 (53%)	0.119 (14%)	1.744 (44%)	0.434 (20%)
$\sigma^2_{wY,h}$	0.494 (23%)	0.214 (24%)	0.622 (16%)	0.227 (10%)
$\sigma^2_{wY,k}$	0.107 (5%)	0.162 (18%)	0.145 (4%)	0.131 (6%)
$\sigma^2_{wY,j}$	0.400 (19%)	0.386 (44%)	1.396 (36%)	1.397 (64%)
Total ( $\sigma^2_{Y,h}$ )	2.125	0.881	3.906	2.189

Legend:  $\sigma^2_{bY,h}$ , variance component between groups;  $\sigma^2_{wY,h}$ , variance component between workers (within-group);  $\sigma^2_{wY,k}$ , variance component within worker (day to day);  $\sigma^2_{wY,j}$ , variance component within worker (within-day).

Table 8. Estimated parameters, exceedances, and probabilities of overexposure for exposures to total particulate matter (TP) and manganese (Mn) for different categories of exposure.

Variable		$\hat{\mu}_{Y,h}$	$\hat{\mu}_{X,h}$	$\hat{\sigma}_{bY,h}^2$	$\hat{\sigma}_{wY,h}^2$	OEL <sub>3</sub> (mg/m <sup>3</sup> )	Exceedance ( $\hat{\lambda}_h$ )	Probability of Overexposure ( $\hat{\theta}_h$ )
TP	US	1.137	6.488	1.001	0.465	5	0.348	0.405
	UK	-0.069	1.943	1.001	0.465	5	0.083	0.074
	Canada	0.438	3.224	1.001	0.465	5	0.167	0.174
	Finland	2.000	15.380	1.001	0.465	5	0.626	0.733
	Manufacturing	1.433	8.726	1.003	0.464	5	0.442	0.522
	Construction	1.252	7.285	1.003	0.464	5	0.384	0.450
	Railroad	1.490	9.242	1.003	0.464	5	0.461	0.545
	Shipyards	0.123	2.354	1.003	0.464	5	0.110	0.105
	Automobile	-0.237	1.644	1.003	0.464	5	0.064	0.054
	Non-specific	0.832	4.788	1.003	0.464	5	0.261	0.293
Mn	US	-2.324	0.525	1.892	1.467	0.2	0.348	0.506
	UK	-3.421	0.175	1.892	1.467	0.2	0.162	0.217
	Canada	-2.618	0.391	1.892	1.467	0.2	0.291	0.421
	Manufacturing	-2.377	0.453	1.674	1.495	0.2	0.333	0.494
	Construction	-3.202	0.198	1.674	1.495	0.2	0.185	0.257
	Railroad	-0.884	2.016	1.674	1.495	0.2	0.658	0.873
	Shipyards	-2.074	0.613	1.674	1.495	0.2	0.397	0.587
	Automobile	-3.629	0.130	1.674	1.495	0.2	0.128	0.163
	Non-specific	-2.251	0.513	1.674	1.495	0.2	0.359	0.533

Legend:  $\hat{\mu}_{Y,h}$ , estimated group mean for logged data, obtained from application of random effects model ( Equation 3) to the logged concentrations (mg/m<sup>3</sup>) grouped by country and industry;  $\hat{\mu}_{X,h}$ , estimated group mean for natural scale data (mg/m<sup>3</sup>);  $\hat{\sigma}_{bY,h}^2$ , between-group variance component, estimated from application of random model ( Equation 3) to the logged concentrations (mg/m<sup>3</sup>) grouped by country and industry;  $\hat{\sigma}_{wY,h}^2$ , within-group variance component, estimated from application of random model ( Equation 3) to the logged concentrations (mg/m<sup>3</sup>) grouped by country and industry.

## **Chapter 3:**

# **Mapping Particulate Matter at the Body Weld Department in an Automobile Assembly Plant**

### **Introduction**

Welders are exposed to high concentrations of welding fumes, which are primarily fine and ultrafine particles. The exposure is associated with increased respiratory symptoms and illness, and potentially cardiovascular diseases, as well as reproductive and neurological effects (Antonini, 2003). The Occupational Safety and Health Administration (OSHA) currently has no permissible exposure limit (PEL) for welding fumes. The PELs for particles not otherwise regulated ( $15 \text{ mg/m}^3$  for total dust and  $5 \text{ mg/m}^3$  for respirable fraction) may not be sufficient to protect workers from the adverse health effects associated with exposure to the fine and ultrafine particles in welding fumes (Hammond et al., 2005; Kim et al., 2005; Park et al., 2006). At the same time, workers' exposures are highly variable, depending on the composition of the metal piece worked on, the welding method employed and the work environment (Burgess, 1995). Ventilation is among the most critical factors influencing airborne particle concentration in a welding workplace; in an insufficiently ventilated workplace exposure levels can be very high.

A cross-sectional study conducted in 2000-2001 in an automobile assembly plant found that welders had increased rates of allergy symptoms, asthma symptoms and cough compared to assembly workers (Hammond et al., 2005). As a result of the study, increasing ventilation and follow-up evaluation were recommended. Subsequently, the ventilation was improved and a follow-up study was conducted to assess the effectiveness of the changes. Particle mapping was performed as part of the follow-up study. Aerosol mapping is a new technique to assess the spatial distribution of an aerosol at a workplace. Particle mapping utilizes direct-reading continuous particle monitors to measure particle air concentrations at pre-determined locations in a sampling grid. This method has been used in several studies to assess the spatial variability in both particle count and mass concentrations (O'Brien, 2003; Dasch et al., 2005; Peters et al., 2006; Heitbrink et al., 2007; Dasch and D'Arcy, 2008; Evans et al., 2008; Heitbrink et al., 2009). Sources for different sizes of particles were identified and effects of process and ventilation on particle size and spatial distributions were evaluated (Dasch et al., 2005; Peters et al., 2006; Heitbrink et al., 2007). Constructed maps were used subsequently to guide control measures and evaluate the efficacy of the controls (O'Brien, 2003). While aerosol mapping appears to be a useful tool for researchers and industrial hygienists to assess particle exposure, its utilization and effectiveness highly depend on mapping method. Mapping data collection grid size, location, sampling interval and the number of replications are the main components of such a method. The study aims will dictate the particular protocols and spatial resolutions needed. For example, when mapping is used as a screening tool to select locations for further intensive monitoring, data can be collected on a relatively coarse grid with a shorter sampling interval (Dasch et al., 2005). However, when the density of processes is high and mapping is expected to generate high resolution spatial maps, the grid size must be sufficiently fine. Although several aforementioned papers have been written in which some mapping method issues were addressed, developing

mapping protocols has not been systematically discussed and the underlying temporal variability has often been neglected in the process of designing a mapping method. During the pilot sampling in this study the need to develop a specific mapping protocol for the body weld department became apparent due to the presence of temporal variations and the characteristics of the operations.

The facility environmental health and safety (EHS) personnel collected two sets of mapping data in the body weld department, one before and one after the ventilation improvements. In the current study, in order to evaluate the effectiveness of the ventilation improvements and the reduction of the particle level, pilot sampling was conducted in June 2005 and intensive mapping data collection sessions were carried out in January 2006. The three specific aims of the study were: first, to develop a mapping protocol specifically for this workplace, with an emphasis on evaluating and incorporating temporal variations in the process of analyzing spatial distributions; second, to explore whether the reduction of particle concentration could be evaluated based on the data collected by the EHS personnel in this facility; and third, to identify potentially high concentration areas and thus to inform further ventilation evaluation, personal monitoring and respiratory health surveys. This manuscript reports the development of the mapping protocol and the results of the mapping.

## **Methods**

### ***Facility/Process Description***

The body weld department had a floor area of approximate 30,000 m<sup>2</sup> and was composed of a car area, a truck area and a suspension area (Figure 1). The car and the truck areas had their own underbody line, side member lines, roof and trunk line, flexible body line and slat line. None of these areas were physically separated or enclosed by any barriers. There were more than 300 evenly spaced steel columns in the body weld department supporting the building structure. Each column was identified by a painted letter/number combination from the plant grid (Figure 1). Operations were usually set up between the columns. Within the major areas, some large robotic welding areas were semi-enclosed by 8-foot tall plastic sheets (not shown in Figure 1) mainly for safety reasons. No manually operated work stations were set up within these enclosed areas. Approximate 300 employees worked in the department on two shifts, the day shift from 6:00am to 2:30pm and the evening shift from 4:30pm to 1:00 am. The plant operated Monday through Friday and closed during the weekend. The facility produced about 900 cars and 600 trucks per day. Day-shifts and evening-shifts were identical as to operations. Although no detailed production rates were obtained for the study period, the overall daily production rate appeared to be consistent and there were no noticeable differences between shifts and days, or between the pilot sampling and the mapping period.

Two types of welding were used in the department: metal inert gas arc welding (MIG) and resistance welding. Robotic welding machines carried out more than 80% of the welding. Numerous ventilation systems were installed throughout the facility to control welding fumes, including local exhaust systems and dilution systems. The local exhaust systems included canopy hoods and enclosing hoods. Canopy hoods were mainly over robotic MIG welding areas while the enclosing hoods were over manual or semi-manual MIG welding operations. The exhausted air was typically routed to cartridge dust collectors (TORIT, Donaldson Torit Corporation,

Minneapolis, MN) adjacent to the welding areas with air passed through filter media and the cleaned air discharged back into the facility. Dilution air supply systems provided outdoor air through numerous inlets located throughout the facility. Many of the air supply inlets were located near the plant ceiling while others were configured to deliver air into the “occupied zone” – 3 to 4 meters above the floor. Welding operations were the primary sources of the airborne particles. Re-suspension from forklift traffic and the discharge from the cartridge dust collectors also contributed to the overall airborne particle concentration. The cartridge dust collectors and an air supply system at the truck slat line were newly installed to increase ventilation as recommended by the original study.

## ***Sampling Instruments***

Multiple instruments were used in the particle sampling. An aerosol photometer with a cyclone, *Personal DataRam* (Model 1200AN, MIE Inc., Bedford, MA), was used to measure particle mass concentration with a size selection of PM<sub>2.5</sub>. The DataRam was equipped with a filter (Teflo Membrane, polytetrafluoroethylene (PTFE) with polymethylpentene support ring, 37mm, Pall Corporation, East Hills, NY) to collect particles for gravimetric analysis. A personal sampling pump (Sidepak Model 550, TSI Inc., Shoreview, MN) was used to draw air through the DataRam at a flow rate of 4 liters/minute. A light scattering direct-reading device, *Microdust Pro Aerosol Monitoring System* (Casella USA, Amherst, NH), was used to measure respirable particle mass concentration. Another light scattering device that was used by the facility EHS personnel collecting mapping data before and after the countermeasures, *DustTrak* (Model 8520, TSI, Inc., Shoreview, MN), was borrowed and used side by side with the *Microdust Pro* for two days during intensive mapping data collection to make comparison between the instruments. An optical particle counter (OPC, PDM-1108, GRIMM Technologies, Inc., Douglasville, GA) was used to assess particle size distribution. The OPC measures particle concentration in either count or mass mode. Data are reported in 15 size channels ranging from 0.23µm to 20µm for mass and 0.30µm to 20µm for count. A built-in pump draws air through the OPC and a 47 mm PTFE filter (Grimm Technologies, Inc., Douglasville, GA) is installed in the OPC to collect particles for gravimetric and chemical analyses. The flow rate is fixed at 2 liters/minute. A condensation particle counter (CPC), *P-Trak Ultrafine Particle Counter* (Model 8525, TSI, Inc., Shoreview, MN), was used to measure fine particle count concentration in a size range of 0.014µm to 1.0µm. Two filter-based cassette samplers were operated in conjunction with the direct-reading instruments: a close-face total particle sampler (SKC, Eighty Four, PA) running at 2 liters/minute and a respirable fraction particle sampler (*Cyclone Assembly*, MSA, Pittsburgh, PA) running at 1.7 liters/minute. Samples were collected on 37-mm diameter Teflo Membrane filters described above. Battery-operated pumps (*Sidepak* Model 550, TSI Inc., Shoreview, MN) were used to draw air through the cassette samplers at the specified flow rates. Instruments were zeroed and spanned following manufacturers’ instructions. All mass concentrations reported in this manuscript that were measured by the direct-reading instruments were gravimetrically corrected. As the DataRam and the OPC both had downstream filters, direct-reading output mass concentrations were corrected by their filter results. Respirable particle mass concentration measured by the *Microdust Pro* and the *DustTrak* was corrected by the filter results of the respirable cassette sampler (*Cyclone Assembly*).

## ***Data Collection***

Pilot sampling was conducted in June 2005. Researchers walked through the facility and collected process related information. Particle concentration was measured during the walkthrough and at selected locations. Temporal variation during a shift was monitored by over-shift stationary sampling using the DataRam and a 1-minute time-weighted average (TWA) log interval at Column M16, a midpoint chosen based on accessibility, minimal inconvenience for the production workers and material handling, and the availability of 120 VAC electrical power. In order to determine an appropriate sampling interval for mapping data collection, particle concentration was measured using the Microdust Pro and a 5-second log interval first at a location near a welding station and then at seven randomly selected locations for 10 minutes at each location to assess the short-term variations. Twenty-second and 1-minute TWAs were calculated based on the data logged every 5 seconds. Coefficients of variation (CVs) for 5-, 20-second and 1-minute TWAs were calculated to evaluate the short-term variability associated with the different sampling intervals. Instruments were also tested during the pilot sampling for their feasibility and stability. A mapping protocol was developed based on the pilot sampling.

Six intensive mapping data collection sessions were conducted in January 2006, three in the day shifts and three in the evening shifts. One session was conducted per day. Each session lasted approximately 8 hours, during which a fixed route traversing 212 selected locations was followed but each session started at a different, randomly selected location. One 1-minute TWA concentration was measured by the OPC, the Microdust Pro and the CPC side-by-side (collocated with the cassette samplers) at each location, identified by the steel columns throughout the department. Data were collected column by column at the column locations, except in large storage areas or at the perimeter of the department where data were collected at every other column. Since the columns were 13 meters apart, one grid point in a constructed map represented an area of 169 m<sup>2</sup>. Mapping data were not collected during the first 30 minutes of a shift, during the breaks or within 20 minutes after the breaks. Over-shift temporal variation was further evaluated using the DataRam at three fixed locations, Columns P03, P13 and M13, selected based on potentially high particle concentrations, types of operation, input from the workers and the accessibility. Due to the availability of the instrument, all the stationary sampling occurred during the evening shifts.

## ***Map Generation***

Data were downloaded from the direct-reading instruments to a computer after each sampling session. Gravimetric correction was performed for mass concentrations based on the filter results. Then the data were matched with the locations and entered into a spreadsheet (Excel, Microsoft Inc.); a contour graphing function was used to generate particle concentration maps. Microdust Pro data were used to construct mass concentration maps for respirable particles. OPC data were used to generate count concentration maps for particles 0.30µm to 20µm. Particle count concentration measured by the CPC was used to construct maps for submicrometer particles in the size range of 0.014µm to 1.0µm. Maps were constructed for each day (not presented in the manuscript), as well as for the arithmetic mean concentrations across multiple sessions for each type of measurement.

## **Statistical Analysis**

Maps for one type of measurement were first graphically examined for the variations across days. Then the data were log transformed and analyzed by repeated measurements one-way analysis of variance (ANOVA) to assess the variations in the spatial distributions across the sessions. The null hypothesis of the ANOVA was that the spatial means (logged) across 212 locations were the same for the six sessions. The ANOVA model can be defined as:

$$Y_{ij} = \ln(X_{ij}) = \mu_Y + b_i + e_{ij} \quad (\text{Model 1})$$

for  $i = 1, 2, \dots, 212$  columns and  $j = 1, 2, \dots, 6$  shifts

where,  $X_{ij}$  represents the particle concentration (1-minute TWA) for the  $i^{\text{th}}$  column on the  $j^{\text{th}}$  sampling session, the response variable  $Y_{ij}$  is the natural logarithm of  $X_{ij}$ ,  $\mu_Y$  represents the true mean particle concentration (logged) over 212 locations across time,  $b_i$  represents the random effect for the  $i^{\text{th}}$  column, and  $e_{ij}$  represents the random deviation of the observed logged particle concentration  $Y_{ij}$  on the  $j^{\text{th}}$  day for column  $i$  from  $\mu_Y$  (i.e.,  $e_{ij} = Y_{ij} - \mu_Y$ ). Under Model 1, it is assumed that  $b_i$  and  $e_{ij}$  are mutually independent and normally distributed, with means of zero and variances  $\sigma_{bY}^2$  and  $\sigma_{wY}^2$ , representing between-column and within-column variations, respectively. Thus, the total variations in logged particle concentration at 212 locations is given by  $\sigma_Y^2 = \sigma_{bY}^2 + \sigma_{wY}^2$ .

Box plot and fitted value vs. residual plot were used to check data distribution and constant variance assumption. Qnorm plot and Shapiro-Wilk test were used to check normality. Tukey's procedure was used for follow-up multiple comparisons to identify where the differences were and if there were any patterns in the differences. Simple arithmetic means of the particle concentrations over 212 locations were also calculated. Chi-square test for trend was applied on the simple arithmetic spatial means to examine the trend through a week. Student's  $t$ -test was conducted using the average and standard deviation of the simple arithmetic spatial means to determine the minimum significant reduction of mass concentration before and after the countermeasures.

## **Results**

This section is composed of two parts: mapping method development and the results of the mapping. The latter includes spatial distributions of mass and count concentrations for particles with different sizes, day-to-day variations in the spatial distribution, and the particle size distribution. Comparison between before- and after-countermeasure is discussed in the next section.

### **Mapping Method Development**

#### **Short-term Variation and Sampling Interval**

Mapping is a time and labor consuming process, especially when the area to be evaluated is large. The sampling interval, defined as the sampling time at each location, has a major effect on the total amount of time required for mapping data collection. When multiple identical instruments are available, an interval of 1-minute is usually used, as identical instruments can be used simultaneously to reduce the sample load (Peters et al., 2006; Heitbrink et al., 2007). In practice, health and safety personnel in a factory usually do not have multiple identical direct-

reading devices, and much shorter intervals such as 5-second or 20-second have been used (Dasch et al., 2005). The EHS personnel in this automobile facility also used a 5-second sampling interval to collect mapping data before and after the countermeasures. During the pilot sampling significant short-term variation was observed, as shown in Figure 2. Particle concentration varied dramatically during welding cycles. Therefore, in order to determine an appropriate sampling interval, we collected data at seven locations for 10 minutes each using a 5-second log interval. The coefficients of variation (CVs) for 5-second, 20-second and 1-minute TWAs were calculated to evaluate short-term variations associated with different sampling intervals (TABLE I). For some locations CVs were small for all sampling intervals, indicating small variations in particle concentration during the sampling periods. For some other locations CVs varied moderately, but the differences between the CVs for the varying averaging times were small. However, there were locations where CVs varied substantially with the CVs for 1-minute TWAs much smaller than those for 5- or 20-second TWAs. These locations were more likely to be within the major operation areas. These results implied that if data were collected for 5- or 20-second intervals at each location during mapping data collection, particle concentration at some locations could vary as much as 67% in 10 minutes. Furthermore, an instrument requires time to respond when it is moved from one location to another. In the pilot sampling 20-30 seconds were needed for the Microdust Pro, the OPC and the CPC to stabilize between readings. Based on these results, a 1-minute sampling interval and a 30-second instrument stabilization time were chosen.

### **Temporal Variation during a Shift**

Temporal variation during a shift was first evaluated at the Column M16 during the pilot sampling and further assessed at the Columns P03, P13 and M13 during the mapping data collection using the DataRam (Figure 1). Reported data were gravimetrically corrected by a factor of 1.52 (gravimetric: direct reading output). The early break and the lunch break were apparent in the temporal plot (Figure 3). The  $PM_{2.5}$  mass concentration decreased 3 fold during the 15-minute early break and 10 fold during the 45-minute lunch break. As the goal of mapping was to assess spatial variations in the particle concentrations, data should be collected during steady-state conditions and thus measurements made during the breaks would not be comparable to those collected during the operations and would lead to underestimation of concentrations at the corresponding locations. Therefore, mapping data were not collected during or within 20 minutes after the breaks, or within 30 minutes of the start of a shift.

After the data collected during these times of low production (“resumption periods”: first 30 minutes of a shift, during and within 20 minutes after a break) were excluded, particle concentration still varied substantially during the work time of a shift (Table II). To better capture this variation and incorporate it into the maps, repeated measurements were necessary. Based on the moderate CV at the Column M16 measured during the pilot sampling, the consistency of the overall operation from day to day observed during the pilot sampling, and the feasibility, we decided to collect mapping data three times on each of two shifts (day-shift and evening-shift). Assuming the difference between the day-shift and the evening-shift was minimal because they were operated identically, the total of six replications were believed to be sufficient to evaluate variations across days. Since there were 212 locations to be evaluated by 1-minute TWAs and data could be gathered only during steady-state periods, an 8-hour work shift could accommodate one mapping data collection event, so only one complete set of samples during

one shift per day was feasible. Therefore, six repeated mapping data collection sessions were carried out on six different days in January 2006. To avoid a location being sampled at the same time during a shift, we designed a fixed route that traversed 212 selected locations. The route was followed in each session, but started at a different, randomly selected location. Data were collected at the column locations rather than between column locations, as the operations were often set up between the columns, thus limiting accessibility. Data were collected at every other column in the large storage area and at the perimeter of the department, as particle concentrations varied little at these locations as observed during the pilot sampling.

## ***Mapping Results***

### **Spatial Variations**

Figure 4 presents a contour map of respirable mass concentration as measured by the Microdust Pro. Each grid point was an arithmetic mean of six mass concentrations collected on six shifts and the data were gravimetrically corrected by a factor of 0.92 (gravimetric: direct reading output) based on the filter results of the respirable cassette sampler. Five “hot spots” appeared on the map, located at Columns U6, N14/P13, T14, N6 and P03. Mass concentrations at these locations are presented in Table III. All the “hot spots” were located in the car area. The arithmetic mean for the car area and the truck area were  $403\mu\text{g}/\text{m}^3$  and  $249\mu\text{g}/\text{m}^3$ , respectively. The mass concentration in the car “under body” area was especially high.

A map of count concentration for particles  $0.30\mu\text{m}$  to  $20\mu\text{m}$  as measured by the OPC (Figure 5) exhibits very similar patterns to those in the map of respirable mass concentration (Figure 4). Data mapped were the arithmetic means of four sessions (OPC was on the mass mode during the other two sessions). All five “hot spots” appeared. However, the particle count concentration at T14 was only about 60% of that at N14/P13; whereas the respirable mass concentration at these two locations were comparable (Table III). Secondly, the “hot spot” at P03 suspension area in the Figure 4 split into two areas, one centered at M02 with a relatively low concentration and the other centered at P03 with a much higher count concentration. The arithmetic means for the car area and the truck area were  $7.0 \times 10^8/\text{m}^3$  and  $4.2 \times 10^8/\text{m}^3$ , respectively.

The patterns of spatial variation presented in the above two maps were barely identifiable in a map of submicrometer particle count concentration as measured by the CPC ( $0.014\mu\text{m}$  to  $1.0\mu\text{m}$ ). The count concentrations in Figure 6 were the arithmetic means of six sessions. Although still relatively high at U6, P03/M02 (suspension) and N14/P13 (car underbody), the submicrometer particle count was much more evenly dispersed and tended to spread over a larger area. No distinguishable peaks appeared at Column T14 and Column N6 in the map. The arithmetic mean was  $1.4 \times 10^{11}/\text{m}^3$  and  $1.1 \times 10^{11}/\text{m}^3$  in the car area and the truck area, respectively. The count concentrations at T14 and N6 were just 1.23 fold of the arithmetic mean count concentration across the 212 locations (Table III). A comparison between peak-to-mean ratios of submicrometer particles and those of larger particles (Microdust Pro and OPC data) indicated that the ratios of the submicrometer particles were much smaller (Table III). In other words, submicrometer particles distributed more evenly across the workplace than the large particles. The ratios of highest 10% concentrations (90<sup>th</sup> percentile) to the mean and highest 10% concentrations to the lowest 10% values (10<sup>th</sup> percentile) are the alternatives of the peak-to-mean ratio and reflect the spatial gradients. While the ratio of 90<sup>th</sup> percentile to 10<sup>th</sup> percentile for large

particle count (0.3 $\mu\text{m}$  - 20 $\mu\text{m}$ ) was 5, it was 3 for submicrometer particles (0.014 $\mu\text{m}$  – 1.0 $\mu\text{m}$ ), further illustrating the more uniform distribution of the submicrometer particles.

### **Day-to-Day Variations of the Spatial Distribution**

Temporal variations could exist within a shift, between the two shifts in a day (day-shift and evening-shift), from day to day and from season to season. Particle concentrations measured during the six sessions in January 2006 were used to assess daily variations, which contained variations between shifts and from day to day within the same season. Results were summarized in Table IV. These two types of variations could not be evaluated separately as the data were not collected during both shifts on the same day due to lack of feasibility. The daily arithmetic spatial mean varied from 305 $\mu\text{g}/\text{m}^3$  to 501 $\mu\text{g}/\text{m}^3$ , with an average of 372 $\mu\text{g}/\text{m}^3$  and a standard deviation (SD) of 71 $\mu\text{g}/\text{m}^3$ . Repeated measurements ANOVA indicated that the spatial means (logged) were statistically different ( $p < 0.0005$ ). Tukey's procedure revealed that the mean of the Jan 5 day-shift was significantly higher than all other means; the means of the Jan. 11 day shift and the Jan. 31 evening shift were significantly higher than those of the Jan. 9 evening shift and the Jan. 23 day shift. Chi-square test for trend further indicated that there was a trend through the week ( $p < 0.05$ ). However, there was no evidence that the day shifts differed from the evening shifts in general.

### **Particle Size Distribution**

The OPC measures particle count or mass concentration in multiple channels. Figure 7 presents the particle size distribution as arithmetic means of four sessions for count and two sessions for mass collected in January 2006. Data were averaged over 212 locations. Particle count median aerodynamic diameter (CMAD) was 0.38 $\mu\text{m}$ . Geometric mean diameter for count concentration was 0.42 $\mu\text{m}$  with a geometric standard deviation (GSD) of 1.32. Ninety-nine percent (99%) of the particles had an aerodynamic diameter smaller than 1.0 $\mu\text{m}$ . These particles accounted for 61% of the particle mass. Meanwhile, particle mass median aerodynamic diameter (MMAD) was 0.85 $\mu\text{m}$  and geometric mean diameter for mass concentration was 1.12 $\mu\text{m}$  with a GSD of 3.33. Respirable and thoracic particles (as defined by American Conference of Governmental Industrial Hygienists (ACGIH) size selective criteria) accounted for 93% and 97% of OPC measured particles, respectively. When the fine particles measured by the CPC (0.014 $\mu\text{m}$  – 1.0 $\mu\text{m}$ ) were considered, 99.99% and 99.5% of the count were particles smaller than 1.0 $\mu\text{m}$  and 0.3 $\mu\text{m}$ , respectively.

## **Discussion**

During the course of using mapping as a method to characterize particle spatial distributions and thus to inform the ventilation evaluation, four types of variations were analyzed: short-term variation (10 minutes in this study) at a fixed location, temporal variation during a shift at each sampling location, spatial variation from location to location (spatial distribution), and the temporal variations of the spatial distributions across shifts and days. Therefore, the research questions became whether mapping could be used effectively to assess particle spatial distributions given the significant temporal variation during a shift at sampling locations; how well a map might represent the spatial distribution across shifts and days; and how particle size might affect assessing particle spatial distribution.

## ***Temporal Variations and Mapping Implications***

It is sometimes assumed that particle concentration is stabilized shortly after an operation resumes. During the data collection in this study we observed that, although the overall production rate was fairly constant across days, the individual production lines were frequently interrupted due to machinery issues and adjustments of the production paces. These interruptions were the major contributors to the fluctuations in the particle concentrations during a shift. The patterns of temporal variation over a shift shown in Figure 3 were similar to those reported by Dasch and D'Arcy for steel resistance welding in other automobile assembly plants (Dasch and D'Arcy, 2008). These variations suggested that, during the mapping data collection, a single data point measured at a random moment during a shift was less likely to represent an 8-hour TWA concentration at a given location, compared to a mean of multiple repeated measurements. The sampling interval selected for a data collection location must consider both the short-term variation and the feasibility of measurement. The average of the repeated measurements needs to be a close approximation of the TWA concentration at a given location over time. Furthermore, due to substantial particle reduction during the breaks, mapping data should not be collected either during or shortly after the breaks.

## ***Variations of Spatial Average and Evaluation of Reduction***

One of the primary goals of mapping in this study was to characterize particle spatial distribution and thus to evaluate the reduction after the countermeasures. Repeated measurements ANOVA identified that the spatial mean (logged) varied significantly from day to day ( $p < 0.0005$ ), indicating that data from a single shift or a single day might not represent particle spatial distribution across days. Graphical examination of the maps from 6 days for respirable mass concentrations revealed missing peaks on some days (data not shown). Repeated measurements over days were necessary for a map to be representative. Moreover, as the six full-shift sessions differed significantly, evaluation of the efficacy of the ventilation countermeasures requires that, rather than comparing the means of particle air concentration measured before and after directly, statistical tests incorporating temporal variations be done to better evaluate the reduction. Two sets of mapping data were collected by the facility EHS personnel using 5-second sampling intervals. Data were collected at 204 locations during both mapping events, with 88% of overlap with the sampling locations selected in the current study. The spatial means were  $273\mu\text{g}/\text{m}^3$  (SD:  $153\mu\text{g}/\text{m}^3$ ) and  $216\mu\text{g}/\text{m}^3$  (SD:  $184\mu\text{g}/\text{m}^3$ ) for data collected before and after the countermeasures, respectively. In the current study, the arithmetic average of the spatial means for the six sets of mapping data was  $372\mu\text{g}/\text{m}^3$ , with a SD of  $71\mu\text{g}/\text{m}^3$ . Since only one set of pre-countermeasure data was available for the comparison, Student's  $t$ -test indicated that the reduction needed to be at least  $191\mu\text{g}/\text{m}^3$  in order to be considered statistically significant, given the sample size of 1 and 6 before and after the countermeasures and with the assumption that the SD was same before and after the countermeasures. The difference between the spatial means of two sets mapping data collected by the facility EHS ( $273\mu\text{g}/\text{m}^3$  and  $216\mu\text{g}/\text{m}^3$ ) was not significant and could not be distinguished from the daily fluctuation of the spatial mean. When the pre-countermeasure data were compared with the data collected in current study, no reduction was indicated. Although fluctuations in the production rate could be a potential explanation, the facts that the pre- and post-countermeasure data were collected using 5-second sampling intervals without replications and data collection was carried out through the breaks

might also result in the underestimation of the concentrations. Therefore, we concluded that the available data were not adequate to evaluate the reduction of the particle concentration. This further emphasized the importance of designing an appropriate mapping protocol. Although the statistical significance is affected by the sample size and may not be the main concern during ventilation evaluation and the goal of exposure reduction should be the best achievable given the technological and feasibility components, temporal variations in particle concentrations should be considered in order to assess the reduction appropriately.

### ***Spatial Variations and Ventilation Conditions***

In this study, five high concentration areas (“hot spots”) were identified by the contour maps. These areas were related to specific ventilation conditions that required further attention. The implications associated with these specific ventilation conditions can be meaningful in other facilities or industrial settings in general. First, our data indicated that the particle concentrations in the car area were much higher than those in the truck area. All five “hot spots” were located in the car area. The car underbody area (Figure 1) was the major sub-area with high concentrations. Ventilation in this area seemed insufficient even after the installation of the cartridge dust collectors. However, the newly installed air supply system at the truck slat line appeared to be effective. Second, in the body weld department, local exhaust ventilation was mainly over MIG welding operations, whereas resistance welding operations were often ventilated by mechanical fans or general ventilation, as they were considered less hazardous. Figure 4 revealed that three out of five “hot spots” were related to resistance welding (Columns U6, T14 and P6/N6). At Column U6 a single resistance welding station was manually operated, running at a pace of 20 minutes in every 60 minutes. No process ventilation was present at this location at the time of sampling; Column T14 was surrounded by a large robotic resistance welding area semi-enclosed by an 8-foot tall plastic sheet wall. Welding was performed most of the time during a shift. Measured particle level was constantly high. An exhaust fan was on the ceiling more than 10m above this location without hoods to capture particles; the area around Columns P6-N6 was similar to that surrounding Column T14. The mapping data were collected outside the plastic sheet and particle concentrations in these enclosed areas could be higher than those measured. Although no employees worked in these enclosed areas and resistance welding is considered less hazardous compared to MIG welding, these areas as well as other similar resistance welding operations were likely to be the major contributors of particles in the facility.

The other two “hot spots”, P13-P14 and P03, were MIG welding areas. Local exhaust enclosures for MIG welding operations did not function equally well at all locations. The welding set-ups in the areas surrounding Column P03 and P13-P14 appeared to resemble the enclosures in suspension MIG welding area (M02-M03) and those at Columns T9-T10, which appeared effective based on particle measurements. Particle concentrations at P03 and P13 were much higher. MIG welding operations were semi-automatic in these areas. Welding was performed inside the enclosures; workers welded parts manually before putting them on the robotic welders. Welding fume leaked from the enclosures while the welding was in process and when automatic roll-down welding screens were pulled up during the parts removal. Each worker performed tasks among several welding stations in close vicinity to the welding operations during the entire shift. Their exposures were most likely even higher than those measured and shown on the map, since the data were collected at the designated mapping data collection locations identified by the physical columns rather than at the work stations. The

facility may need to identify why the enclosures in the P03 and P13 areas were not controlling particles as effectively as they did at Column T9-T10. High concentration areas where workers were present, such as Columns P03 and P13, are potential locations to conduct personal monitoring to better characterize workers' exposure when it is possible.

### ***Particle Size Distributions***

The OPC data showed that the GSDs for count and mass distributions differed substantially, suggesting a bimodal distribution with other sources for larger particles. Our data indicated, in the body weld department, respirable particle mass concentration was more than two times higher than the levels found in other similar automobile assembly facilities (Dasch and D'Arcy, 2008). Moreover, the percentages of respirable and thoracic particles (93% and 97%) were much higher than those reported by Dasch and D'Arcy (54% and 61%). Besides the production rate, the density of welding operations and the efficiency of the ventilation systems might explain the differences. We found that small particles distributed more uniformly across different processing areas than the larger particles did. A comparison of the respirable mass map (Figure 4) with that of submicrometer particle count (Figure 6) revealed a smaller spatial gradient of the latter, which was also illustrated by the map for the submicrometer particle count having smaller peak-to-mean ratios, as well as smaller ratios of 90<sup>th</sup> percentile to 10<sup>th</sup> percentile (Table III) compared to the maps of larger particles. These findings reflect the fact that submicrometer particles are both more readily transported with air currents and less likely to settle, and thus more uniformly distributed in a facility, as found in other studies (Peters et al., 2006; Evans et al., 2008). When the map of mass concentrations (Figure 4) was compared to those of count concentrations (Figure 5 & 6), the "hot spot" surrounding P03 split into two areas (P03 and M02) in both count concentration maps (0.30 $\mu$ m-20 $\mu$ m and 0.014 $\mu$ m-1.0 $\mu$ m), which implied that the local exhaust ventilation in the suspension MIG welding area surround M02 functioned more effectively in capturing larger particles, while a significant fraction of small particles, especially submicrometer particles, were still emitted from the processes. This is consistent with Dasch and colleagues' finding of enclosed and vented processes shifting particle size distribution to smaller particles (Dasch et al., 2005). These findings emphasize that, (1) ventilation systems should be evaluated not only by reduction on mass concentration but also on count concentration, especially for welding processes that are known to generate fine and ultrafine particles; (2) emission from less hazardous welding operations such as resistance welding should also be effectively controlled. Those who work in areas with less welding activities and thus are predicted to have low exposures may be exposed to fine particles at levels higher than has traditionally been thought. Therefore, removal of fine and ultrafine particles from a facility is more important than blowing them away from the emission sources. Exposures of those who do not work in close vicinity of the emission sources should also be evaluated when assessing workers' exposure to fine and ultrafine particles.

### **Conclusions**

Aerosol mapping is a newly emerging method. Although there are not many publications on this specific topic, mapping has been used both in the practice of industrial hygienists and in exposure studies by occupational health researchers. The concept of mapping can go beyond measuring particles or aerosols. Mapping protocols need to be developed according to the study

aims and the characteristics of the processes and the facility. The following issues were considered in the process of developing the mapping protocol used in this study:

- Grid size, adjusted according to the facility layout, process density and particle emission strength that influence the spatial variations;
- Sampling locations, chosen based on accessibility but preferred to be as close to the workstations as possible;
- Sampling interval at data collection locations, determined by the short-term variation and the feasibility;
- Sampling time frame, selected to avoid collecting data during “resumption periods”; and
- Replications, determined by the magnitude of temporal variations during a shift and across shifts/days.

The particle concentrations in the body weld department had moderate over-shift temporal variation and significant spatial variations. The day-to-day variations in the spatial means were statistically significant. Following a mapping protocol developed specifically for this workplace, we found that, 1) particle concentrations in the car area, especially in the car underbody area, were much higher than those in the truck area; ventilation in the car underbody area seemed insufficient even after countermeasures were taken; 2) local exhaust enclosures for MIG welding operations did not function equally well at all locations; the facility may need to identify the reasons and higher level of controls may be needed in some areas where high concentrations occurred; 3) although resistance welding is considered less hazardous than MIG welding, the resistance welding operations could be the major particle emitting sources if not effectively controlled; 4) submicrometer particles were more evenly distributed across the facility compared to the larger particles and thus workers not in the close vicinity of intensive welding operations might be exposed to fine particles at levels higher than have been traditionally thought; 5) the available data were not adequate to evaluate particle level reduction, indicating that a well-designed mapping protocol is critical in order to achieve the purposes of the study.

## References

- Antonini JM. (2003) Health effects of welding. *Critical Reviews in Toxicology* **33**: 61-103.
- Burgess WA. (1995) *Recognition of Health Hazards in Industry; A Review of Materials and Processes*. 2nd New York: John Wiley & Sons. ISBN 0 471 57716 2.
- Dasch J, D'Arcy J, Gundrum A, Sutherland J, Johnson J, Carlson D. (2005) Characterization of fine particles from machining in automotive plants. *Journal of Occupational and Environmental Hygiene* **2**: 609-625.
- Dasch J, D'Arcy J. (2008) Physical and chemical characterization of airborne particles from welding operations in automotive plants. *Journal of Occupational and Environmental Hygiene* **5**: 444-454.
- Evans DE, Heitbrink WA, Slavin TJ, Peters TM. (2008) Ultrafine and respirable particles in an automotive grey iron foundry. *Annals of Occupational Hygiene* **52**: 9-21.
- Hammond SK, Gold E, Baker R, Quinlan P, Smith W, Pandya R, et al. (2005) Respiratory health effects related to occupational spray painting and welding. *Journal of Occupational and Environmental Medicine* **47**: 728-739.
- Heitbrink WA, Evans DE, Peters TM, Slavin TJ. (2007) Characterization and mapping of very fine particles in an engine machining and assembly facility. *Journal of Occupational and Environmental Hygiene* **4**: 341-351.
- Heitbrink WA, Evans DE, Ku BK, Maynard AD, Slavin TJ, Peters TM. (2009) Relationships Among Particle Number, Surface Area, and Respirable Mass Concentrations in Automotive Engine Manufacturing. *Journal of Occupational and Environmental Hygiene* **6**: 19-31.
- Kim JY, Chen J-C, Boyce PD, Christiani DC. (2005) Exposure to welding fumes is associated with acute systemic inflammatory responses. *Occupational and Environmental Medicine* **62**: 157-163.
- O'Brien DM. (2003) Aerosol Mapping of a Facility with Multiple Cases of Hypersensitivity Pneumonitis: Demonstration of Mist Reduction and a Possible Dose/ Response Relationship. *Applied Occupational and Environmental Hygiene* **18**: 947-952.
- Park RM, Bowler RM, Eggerth DE, Diamond E, Spencer KJ, Smith D, et al. (2006) Issues in neurological risk assessment for occupational exposures: The Bay Bridge welders. *Neurotoxicology* **27**: 373-384.
- Peters TM, Heitbrink WA, Evans DE, Slavin TJ, Maynard AD. (2006) The mapping of fine and ultrafine particle concentrations in an engine machining and assembly facility. *Annals of Occupational Hygiene* **50**: 249-257.

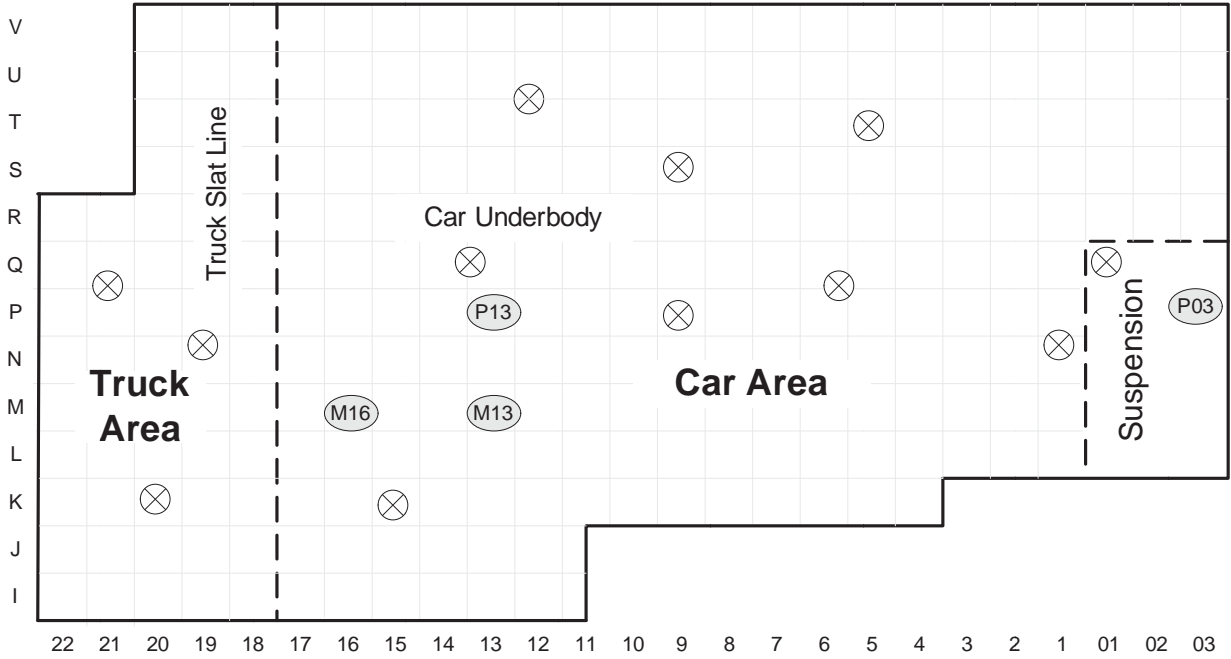


FIGURE 1. Facility layout of the body weld department. The gray dashed lines delineate the main areas defined by the facility based on operations/ activities. ● location for stationary monitoring over a shift. Locations are identified by letter/number combinations from the plant grid (columns are 13 m apart); ⊗ cartridge dust collector

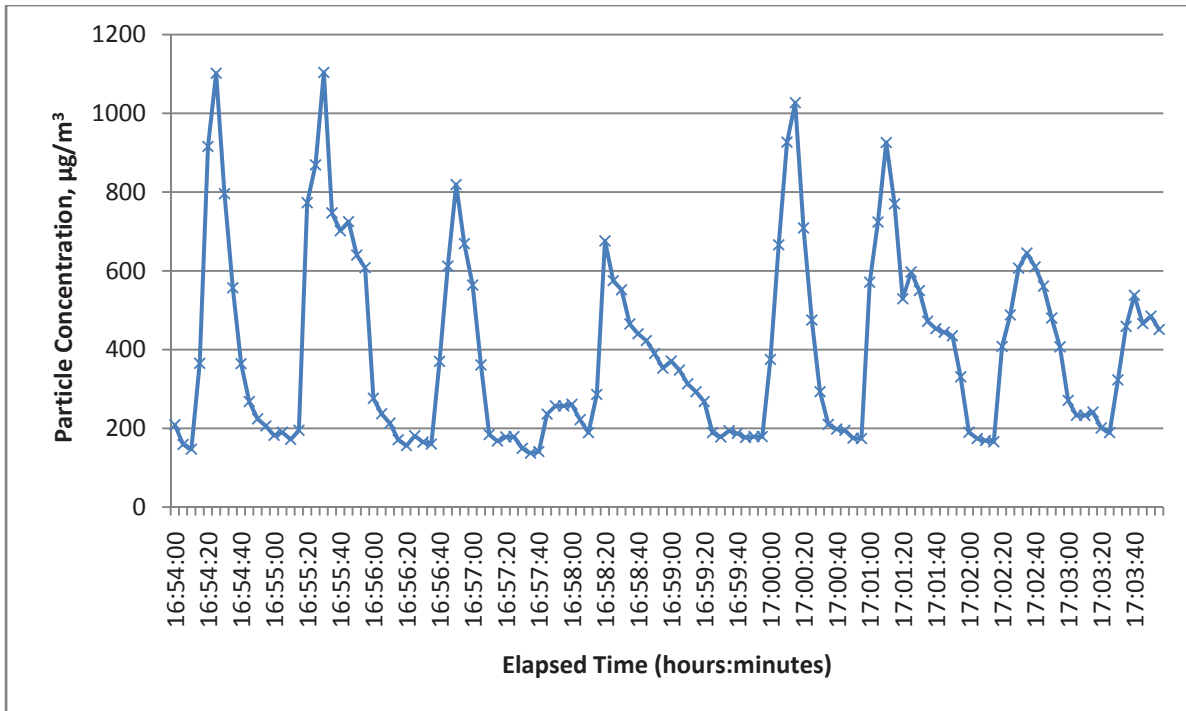


FIGURE 2. Short-term variation at a fixed location (Column M02), measured by Microdust Pro

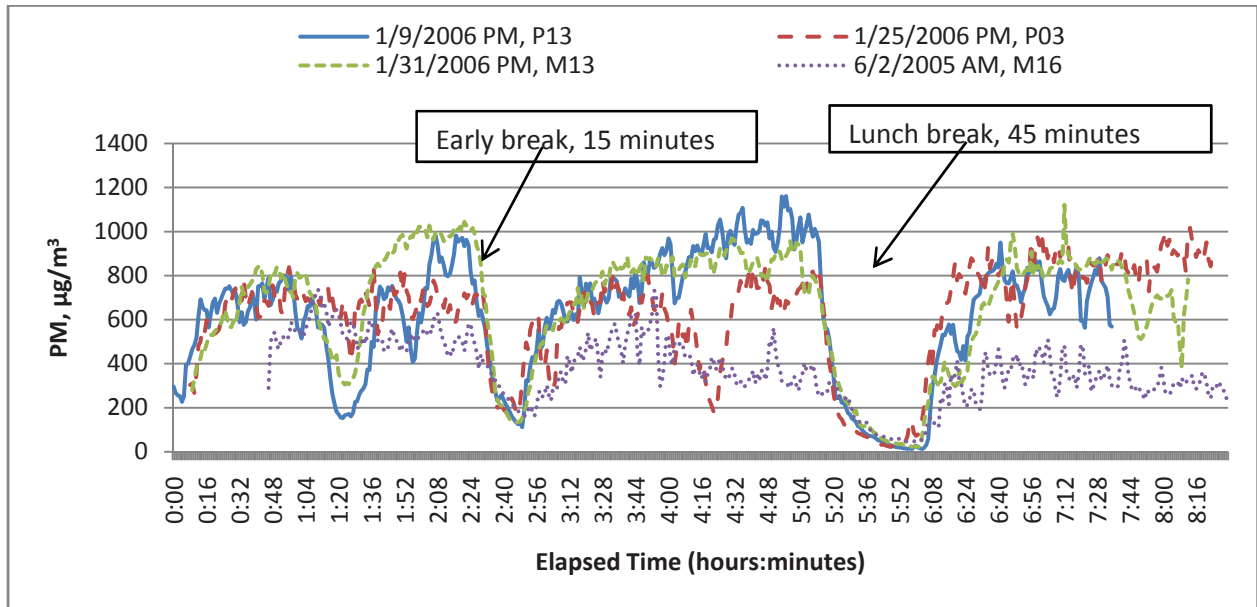


FIGURE 3. Over-shift temporal variation at fixed locations, measured by DataRam

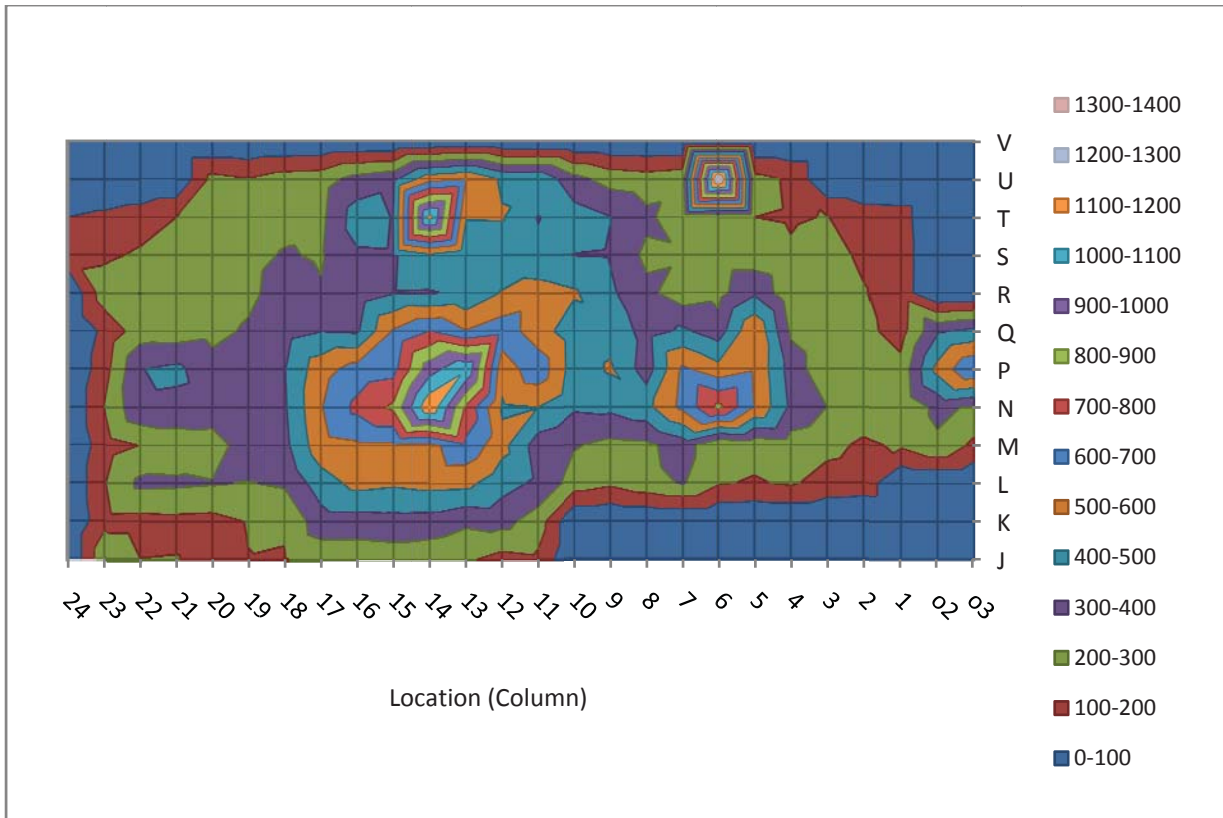


FIGURE 4. Respirable particle mass concentration, measured by Microdust Pro,  $\mu\text{g}/\text{m}^3$

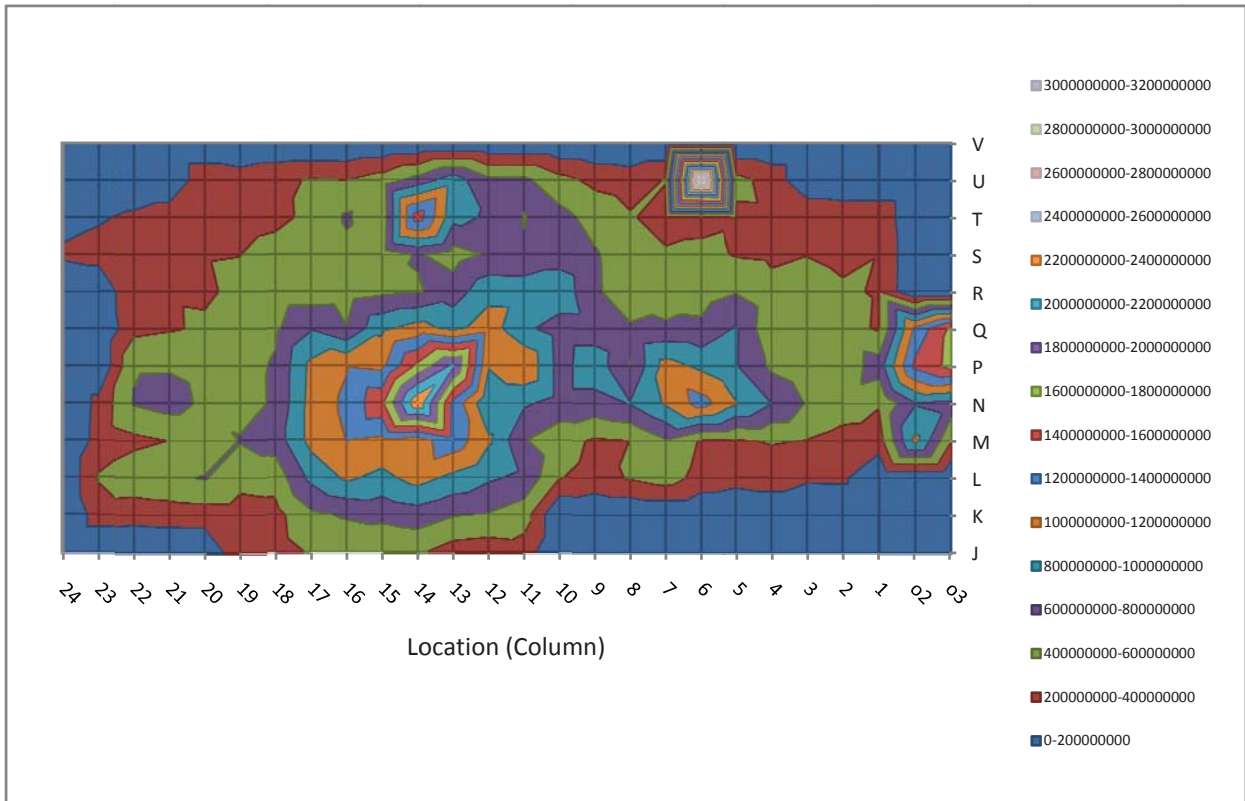


FIGURE 5. Particle count concentration, measured by OPC (0.30µm - 20µm), /m<sup>3</sup>

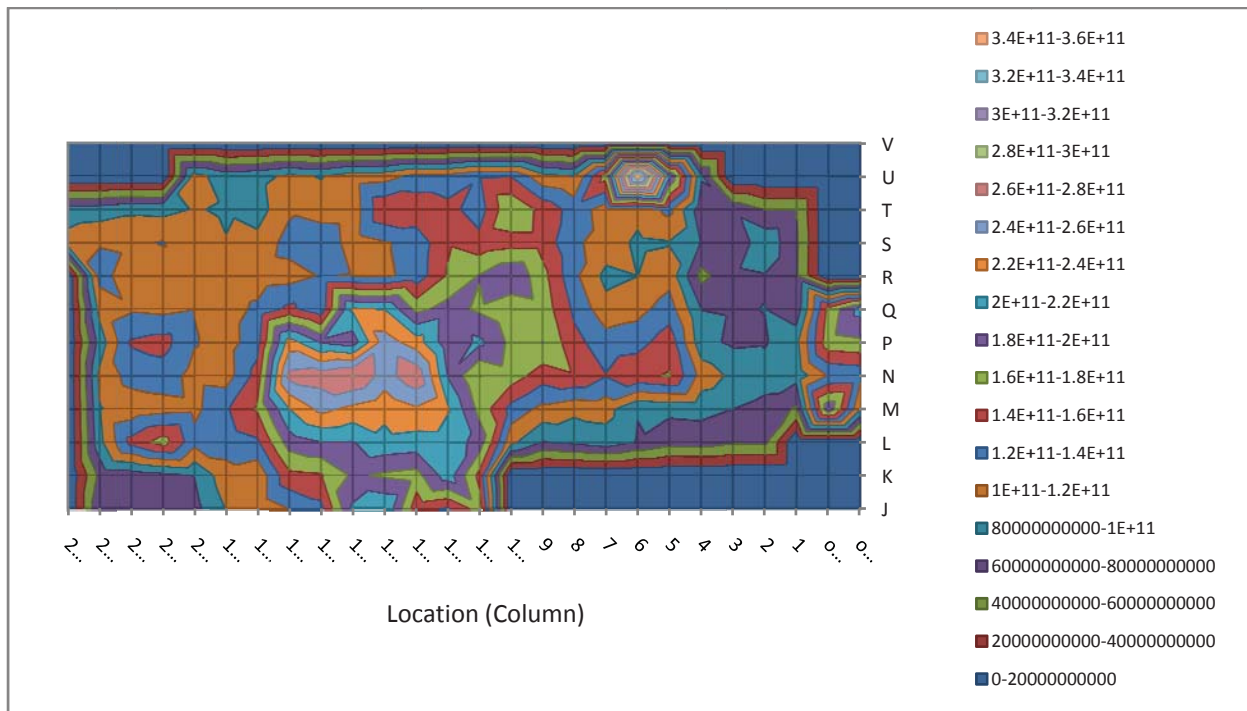


FIGURE 6. Submicrometer particle count concentration, measured by CPC ( $0.014 \mu m - 1.0 \mu m$ ),  $/m^3$

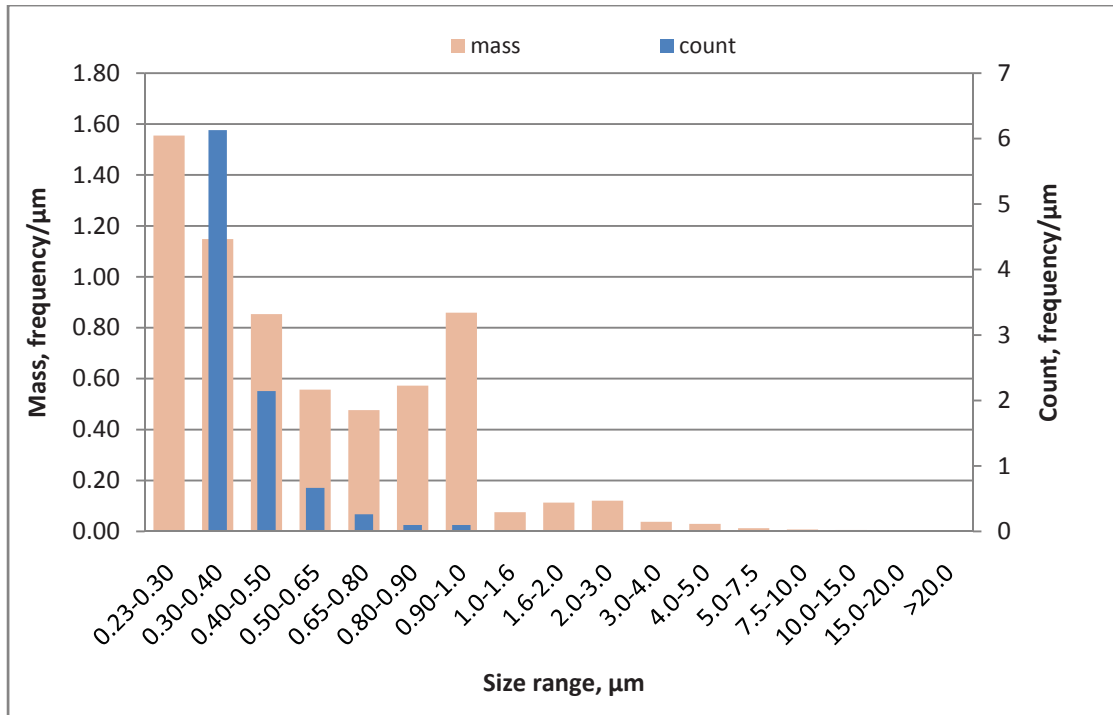


FIGURE 7. Particle mass (0.23 $\mu\text{m}$  to 20 $\mu\text{m}$ ) and count (0.30 $\mu\text{m}$  to 20 $\mu\text{m}$ ) distributions as functions of particle size, measured by OPC

TABLE I. Coefficients of Variation (CVs) for Different Sampling Intervals at Multiple Locations

<u>Location</u>	<u>5-second</u>	<u>20-second</u>	<u>1-minute</u>
L5	0.06	0.05	0.04
T20	0.07	0.06	0.05
N14	0.15	0.13	0.12
N5	0.16	0.16	0.17
Q20	0.24	0.20	0.18
P03	0.51	0.41	0.26
M02	0.67	0.60	0.28

TABLE II. Over-Shift Temporal Variation at Fixed Locations (unsteady-state periods excluded), measured by DataRam,  $\mu\text{g}/\text{m}^3$

Date	Location	Shift	TWA	SD	CV
6/2/2005	M16	day	399	122	0.30
1/9/2006	P13	evening	734	196	0.27
1/25/2006	P03	evening	707	149	0.21
1/31/2006	M13	evening	757	177	0.23

TABLE III. Particle Concentrations at Specific Locations

High Concentration Area	Respirable Particle Mass		Particle Count (0.30 $\mu$ m - 20 $\mu$ m)		Particle Count (0.014 $\mu$ m - 1.0 $\mu$ m)	
	Concentration, $\mu$ g/m <sup>3</sup>	Ratio to Mean	Concentration, m <sup>-3</sup>	Ratio to Mean	Concentration, m <sup>-3</sup>	Ratio to Mean
U6	1330	3.58	3.1x10 <sup>9</sup>	4.92	3.6x10 <sup>11</sup>	2.77
N14	1127	3.03	2.4x10 <sup>9</sup>	3.81	2.8x10 <sup>11</sup>	2.15
T14	1182	3.18	1.5x10 <sup>9</sup>	2.38	1.6x10 <sup>11</sup>	1.23
N6	819	2.20	1.3x10 <sup>9</sup>	2.06	1.6x10 <sup>11</sup>	1.23
P03	697	1.87	1.7x10 <sup>9</sup>	2.70	2.0x10 <sup>11</sup>	1.54
Arithmetic mean over 212 locations	372		6.3x10 <sup>8</sup>		1.3x10 <sup>11</sup>	
90 <sup>th</sup> percentile /mean		2.1		2.4		1.8
90 <sup>th</sup> to 10 <sup>th</sup> percentile		4.5		5.2		3.3

TABLE IV. Spatial Mean & Variation of Respirable Particle Mass Concentration, measured by Microdust Pro,  $\mu\text{g}/\text{m}^3$

Date	Day of Week	Shift	n	Mean	SD	CV	Range
5-Jan	Thursday	day	212	501	462	0.92	94 - 4517
9-Jan	Monday	afternoon	212	310	202	0.65	16 - 1719
11-Jan	Wednesday	day	212	384	193	0.50	98 - 1319
23-Jan	Monday	day	212	305	176	0.58	86 - 952
25-Jan	Wednesday	afternoon	212	357	145	0.41	153 - 970
31-Jan	Tuesday	afternoon	212	377	239	0.63	94 - 1519

## Chapter 4:

# Manganese Exposure and Size Distribution in Welding Fumes in three Chinese Factories

## Introduction

Manganese is a common component in welding materials. It is used in steel alloys to improve metallurgical properties and provide both strength and hardness to the metal. Manganese is also an alloying element in non-consumable welding electrodes, as well as in consumables, with electrodes containing 0.4% to 15% of manganese. Manganese in welding material provides deoxidizing reactions and minimizes weld impurities (Santamaria et al., 2007). It is estimated that there are 1 million full-time and 5 million part-time welders worldwide. Given a variety of types of welding processes and their wide range of applications, welders are probably the largest occupation group exposed to airborne manganese. However, welders' exposures to manganese and potential neurological effects have not been well-assessed. Studies evaluating welders' neurological health status often provide very limited or no exposure data (Santamaria et al., 2007). The number of exposure studies is sparse and few of them assessed the association between manganese air concentration and process type, material composition, work load or ventilation.

Moreover, manganese is usually measured in total and/or respirable particles in exposure studies. Manganese distribution in different sizes particle has not been evaluated. The distribution of manganese as a function of particle size greatly affects its penetration, deposition and absorption in the respiratory track and thus its toxicity. Welding fumes are primarily fine particles smaller than  $1\mu\text{m}$ , which may be more toxic than larger particles (Araujo and Nel, 2009; Lippmann and Chen, 2009; Madl and Pinkerton, 2009; Samuelsen et al., 2009; Schmid et al., 2009). Studies have shown that ultrafine particles ( $<0.1\mu\text{m}$ ) may be rapidly translocated into the brain through olfactory transportation bypassing the blood-brain barrier (Tjalve and Henriksson, 1999; Brenneman et al., 2000; Antonini, 2006). This is particularly important to manganese neurotoxicity through inhaling welding fumes, as manganese primarily targets the central nervous system and welding fumes are small. Size-selective air concentrations of manganese have been shown to be important to its toxicity in epidemiology studies. Iregren (1990) found that manganese in respirable particles but not in total ones was correlated with foundry workers' performance on neurological tests (Iregren, 1990). Ellingsen et al. (2003) assessed workers' exposure to inhalable and respirable manganese in manganese alloy production plants. Manganese in respirable particles, but not in inhalable particles, was found to be associated with manganese in urine (Ellingsen et al., 2003). However, manganese distribution in welding fumes, especially in fine/ultrafine welding particles, has not been investigated.

On the other hand, welders' exposures are difficult to assess. Welders are a heterogeneous working population, mainly due to the large number of welding processes and their wide applications in different industrial settings. Their exposures are highly affected by the welding process utilized, welding rate, material worked with and most importantly the work environment. Efforts have been made to characterize welders' wide range of exposure to

manganese. For example, OSHA conducted monitoring for manganese in welding fumes from 1990 to 2000 and obtained more than 7000 manganese air concentration measurements, categorized as from all job titles containing “welding”, in steel fabrication shops, and in pressure vessels and shipyards. Average manganese air concentration was reported as  $270\mu\text{g}/\text{m}^3$ . Similarly, industrial hygienists in the US Navy and the electric power generation industry collected a large amount of data on exposure to metals during welding, including manganese. The association between manganese air concentration and potential determinants such as process/work environment conditions has not been well assessed. These exposure determinants are crucial not only to particle and manganese air concentrations, but also to their size distributions, an exposure characteristic that fundamentally influences the toxicity of particle and manganese. In order to assess welders’ exposures, with emphasis on manganese in fine and ultrafine particles, this study was conducted to analyze manganese air concentration and size distribution from common welding processes. The specific aims were: 1) to determine to what extent manganese in welding fumes was associated with submicrometer particles ( $< 0.1\mu\text{m}$ ); and 2) to examine how manganese air concentration and size distribution were associated with welding process type, material, work load and work environment.

## Methods

### *Identifying welding processes and facilities*

Among 80 welding processes listed by the American Welding Society (AWS), some processes are more important relative to others based on their widespread use and potential for significant manganese exposure. These processes include, but are not limited to, shielded metal arc welding (SMAW), flux core arc welding (FCAW), gas tungsten arc welding (GTAW), gas metal arc welding (GMAW), submerged arc welding (SAW), plasma arc welding (PAW), laser welding and resistance welding (Burgess, 1995). During welding, manganese air concentration is largely dictated by the fume generation rates (FGRs) as well as welding material composition and workload. Table 1 gives examples of FGRs for shielded metal arc welding and gas metal arc welding when different electrodes are used in welding mild steel (AWS, 1979). Studies have shown when these two type of welding are used to weld mild steel, manganese is a principle element in the fumes, ranging from 3% to 10%, second only to iron (Burgess, 1995). Joint efforts were made by the investigators of this study and Chinese collaborators to identify accessible welding places. As a result, three factories in southern China were identified and access was obtained. The first factory (Factory A) was a manufacturer of boiler components that were later to be assembled at power plant construction sites; the second factory (Factory B) produced steel structures for building construction; and the last one (Factory C) produced hydraulic turbines. These three medium size factories had floor areas ranging approximately from  $1500\text{m}^2$  to  $6000\text{m}^2$ . The types of welding processes used in these factories were shielded metal arc welding, gas metal arc welding, submerged arc welding and plasma arc welding. The density of welding operations was low in these facilities at the time of sampling. Working hours were from 8am to 5pm with a 1-hour lunch break. Job tasks were performed intermittently with welding time ranging from 20% to 60% of the shift time.

## ***Sampling Instruments***

Three types of samplers were used, cassette total and respirable samplers and multi-stage impactor samplers. The samples of Mn in total particles and in respirable particles were collected because, (a) they are commonly used to assess exposures in existing studies; (b) they are appropriate to provide profiles of exposure levels; (c) they are the matrices of the occupational standards; and (d) the ratio of respirable Mn to total Mn is a prelude index of manganese size distribution before further examination of detailed size distribution by impactors. Total and respirable particle samples were collected using plastic cassette samplers following OSHA method PV2121 and SLC1: a closed-face total particle sampler (SKC, Eighty Four, PA) with a flow rate of 2 L/min, and a respirable fraction particle sampler (*Cyclone Assembly*, MSA, Pittsburgh, PA) with a flow rate of 1.7 L/min. Sampling media were 37-mm diameter mixed cellular ester filters (MCE 225-9, SKC, Eighty Four, PA). Battery-operated pumps (*Sidepak Model 550*, TSI Inc., Shoreview, MN) drew air through the cassette samplers at the specified flow rates.

Manganese in fine and submicrometer particles was sampled using multi-stage impactors (Soiutas, SKC, Eighty Four, PA) with cut-points of PM<sub>2.5</sub>, PM<sub>1.0</sub>, PM<sub>0.5</sub> and PM<sub>0.25</sub>. Thirty seven-mm diameter mixed cellular ester filters (MCE 225-9, SKC, Eighty Four, PA) were used as collection substrate and a PTFE filter (Teflo Membrane, polytetrafluoroethylene (PTFE) with polymethylpentene support ring, 37mm, Pall Corporation, East Hills, NY) was used as the after-filter to collect particles smaller than 0.25 $\mu$ m. A pump with flow capacity 5 - 15 liter per minute (Leland Legacy Sample Pump, SKC, Eighty Four, PA) was used to draw air through the impactor at a flow rate of 10 L/min as required by the impactor. PTFE filters were used as the after-filter (instead of MCE filters) because they have one third of the filter back pressure that MCE filters do, which is 4.75 inch of H<sub>2</sub>O for PTFE and 12.5 inch of H<sub>2</sub>O for MCE, respectively, at flow rate of 4 liter/minute. Filter back pressure information for these two types of filters at the flow rate of 10 L/min was not available. When MCE filters were used as an after-filter in instrument testing, the pump automatically shut down due to excessive back pressure.

## ***Data collection***

Data were collected in March 2008 with 5 days in Factory A, 3 days in Factory B and 1 day in Factory C. Three to five welding sites were selected for each welding process. Full-shift samples were collected to obtain 8 hr TWAs. Sampling was continued during morning and afternoon breaks as workers remained in the shops while it was discontinued during the lunch break. Total and respirable samples were collected side by side. Impactor samples were collected collocated with some of the total/respirable pairs, as only two multi-stage impactors were available. Each impactor was accompanied by a pair of total/respirable samples. Both breathing zone and area samples were collected. A breathing zone sample was collected by a sampler held by a researcher in a welder's breathing zone as a surrogate of a personal sample. As there were only two researchers working on site during data collection, only two sets of breathing zone samples were collected during a day. Other samples from that day were area samples that were located as close as possible to a welder to represent the welder's exposure approximately. Because the sample size was small and the area samples were all collected in the near field, the breathing zone samples and area samples were combined in data analysis. The multi-stage impactor samples were always collected as breathing zone samples. A total of 106 samples were

collected during 9 days of sampling in the three factories for four types of welding processes, including 45 pairs of total and respirable samples, and 16 multi-stage impactor samples (Table 2).

The original plan to collect information on exposure covariates associated with measurements is presented in Table 3. However, this was adjusted based on several observations during data collection. Only one type of base metal was used in each factory: mild steel in both Factory A and Factory B, and stainless steel in Factory C. Thus, consumables used in factory A and B were the same, and they were slightly different from what was used in the Factory C. Operation parameters (voltage, current and wire feeding rate) for a given welding process had very similar settings across factories, implying that standardized operation guidelines might have been followed. The work environment was highly similar in these factories. The density of welding operation was low. No local exhaust ventilation was observed during sampling. Natural ventilation was gained from high ceilings, numerous windows and widely opened doors. Therefore, exposure covariates to be investigated were focused on process type, welding consumables, and workload (welding time).

### ***Analytical method***

All filters (MCE and PTFE) were first analyzed gravimetrically to obtain mass of particle collected on each filter and then to obtain size selective particle air concentrations. The filters were analyzed chemically to obtain metal composition of the particles. Chemical analysis was performed using Inductive Coupled Plasma Optical / Atomic Emission Spectrometer (ICP OES/AES), according to OSHA Standard Method 7303 (Elements by ICP Hot Block/HCl/HNO<sub>3</sub> Digestion). Metals examined were aluminum (Al), calcium (Ca), cadmium (Cd), cobalt (Co), chromium (Cr), copper (Cu), iron (Fe), lead (Pb), manganese (Mn), nickel (Ni), and titanium (Ti). Reagent blanks and media blanks were analyzed in the same way as for the samples.

## **Results**

### ***Particle and manganese exposure levels***

The summary statistics for PM and Mn concentrations are presented in Table 4. Cumulative distribution plots are shown in Figure 1. Wide ranges of exposure were observed. Coefficients of variation were above 170% for all agents. The Chinese Occupational Exposure Limit for welding fumes is 4mg/m<sup>3</sup> as 8hr TWA for total particulate matter, and it is 0.15mg/m<sup>3</sup> for Mn in total particles. Whereas US OSHA PELs are 15 mg/m<sup>3</sup> for TP and 5 mg/m<sup>3</sup> for respirable particles, and ACGIH TLVs are 0.2mg/m<sup>3</sup> (current) and 0.02mg/m<sup>3</sup> (proposed) for Mn in total and respirable particles, respectively. Over 20% of TP and Mn in TP measurements exceeded respective Chinese OELs, and the percentages of the measurements for respirable particles and Mn in respirable particles exceeding the respective TLVs were 18% and 52%, respectively.

When the measurements were stratified by process, shielded metal arc welding operations produced the highest concentrations, with AMs (of 8-hr TWAs) of 3.28 mg/m<sup>3</sup> and 2.20 mg/m<sup>3</sup> for total and respirable PM, and 0.14 mg/m<sup>3</sup> and 0.11 mg/m<sup>3</sup> for total and respirable Mn (Figure 2). These levels were 6-fold and 4-fold higher than PM and Mn concentrations resulting from plasma arc welding (0.59 mg/m<sup>3</sup> total and 0.38 mg/m<sup>3</sup> respirable for PM, and 0.032 mg/m<sup>3</sup> total and 0.028 mg/m<sup>3</sup> respirable for Mn). When stratified by factories, concentrations in Factory C

appeared to be higher than those in the other two factories, particularly for Mn exposures (Figure 3).

### ***Particle size distribution***

Particle size distribution was evaluated by data from both cassette samplers and impactor samplers. On average, respirable particles accounted for 56% of total particles (averaged across processes and factories). When averaged by process across factories, the ratio of respirable to total particle air concentrations ranged from 37% to 67% (Table 5). Impactor data revealed that overall, 66% of total particle mass was distributed in particles smaller than 0.5 $\mu$ m.

### ***Manganese size distribution***

Manganese size distribution was assessed by Mn in total and respirable particles, as well as by Mn in different size ranges of particles measured by the impactor sampler. When measured Mn air concentrations in respirable particles were compared to those in total particles, overall, Mn in respirable particles accounted for 63% of Mn in total particles (averaged across processes and factories) (Table 6). Among the processes examined, particles generated from plasma arc welding had the highest percentage of Mn in respirable particles (over 86%), while particles from submerged arc welding had the least (27%). Impactor data revealed that over 82% of Mn mass was distributed in particles smaller than 0.5 $\mu$ m, with plasma arc welding having the highest percentage (97%) and submerged arc welding having the least (55%).

Mn distribution was further assessed by the Mn percentage of particle mass, which was calculated for each size range measured by the impactor. The results (Table 7) indicated that the Mn percentage of particle mass was the highest in the smallest size range (particles <0.25 $\mu$ m). This percentage decreased as particle size increased, becoming the smallest in the largest size range (> 2.5 $\mu$ m). This pattern was consistent across the processes, except for submerged arc welding. But the gradient varied by process. Again, plasma arc welding had the largest contrast, with Mn percentage of particle mass in particles smaller than 0.25 $\mu$ m over 20-fold higher than that in particles larger than 2.5 $\mu$ m. Submerged arc welding had the least contrast.

When the comparison was made between particle size distribution and Mn size distribution among processes, the contrast between PM and Mn mass distributions varied by process (Figure 4). For shielded metal arc welding and submerged arc welding, Mn mass distributions in different size ranges were similar to those of PM. However, for gas metal arc welding and plasma arc welding, the Mn mass distributions differed considerably from those of PM. Substantially larger percentage of Mn mass was distributed in the size range of <0.5 $\mu$ m for gas metal arc welding and plasma arc welding (87% and 97%), compared to PM (65% and 62%). These two processes were the major contributors to the overall difference between PM and Mn mass distributions across processes and factories (Table 6).

## **Discussion**

### ***Exposure levels***

Average PM and Mn air concentrations varied over 6-fold and 4-fold by process, respectively (Figure 2). Shielded metal arc welding had relatively high PM and Mn air

concentrations compared to gas metal arc welding and submerged arc welding. Plasma arc welding had the lowest concentrations. This finding is consistent with what is known about these processes (Burgess, 1995). There were considerable variations in the measurements, indicated by the wide ranges of measured concentrations and the standard deviations. This might be due to the variability of the workload across sampling sites within and between factories. Over 20% of TP and Mn in TP measurements exceeded Chinese OELs, and 18% and 52% of measurements exceeded the respective TLVs for respirable particles and Mn in respirable particles, respectively, for which there are no Chinese OELs. These findings suggested that exposures to PM and Mn in these factories might be of concern.

### ***Mn size distribution***

Manganese in respirable PM accounted for 63% of Mn in total PM, while respirable particles accounted for only 56% of total particles, indicating Mn was more concentrated in respirable particles. This was further confirmed by data from the impactors. Compared to PM mass distribution, more Mn mass was distributed in the size range smaller than 0.5 $\mu$ m. Our research questions began with how Mn was distributed in different sizes of particles in welding fumes. We wanted to know if Mn was evenly distributed in different sizes of particles, and specifically, whether there was a significant amount of manganese associated with submicrometer or ultrafine particles. Data from the multi-stage impactors revealed that both Mn mass fraction (of total manganese mass) and Mn percentage of particle mass increased substantially in particles smaller than 0.5 $\mu$ m. As a result, depending on the process, 55% (SAW) to 97% (PAW) of total manganese mass was distributed in these submicrometer particles (Figure 4). This finding is of great significance. It means, in the measured size range, not only the mass of particles increased with decreasing size, a characteristic of welding fumes, but the percentage of that mass due to manganese increased as well. Given the exponentially increasing surface area with decreasing particle diameter, the bioavailability of manganese in the submicrometer particles could be much greater. Moreover, small particles in the nano-size range may have a higher potential to penetrate into the blood stream from the lungs and thus reach the brain. Small particles in the nano-size range may also reach the brain via olfactory transportation bypassing the blood-brain barrier. As manganese toxicity primarily affects the central nervous system, the finding of Mn enriched in submicrometer particles in welding fumes may imply that welders' risk of developing neurological effects due to exposures to manganese may be potentially higher than it had been traditionally thought. Because welders' exposures to manganese in total welding fumes appear to be lower than exposures in high-exposure occupational settings such as mine, ore processing plants, etc., welders have been considered as low risk manganese exposed occupational group. However, if Mn does enrich in small particles and olfactory transportation does play an important role in manganese neurotoxicity, welders' exposure should be carefully re-evaluated.

### ***Effects of process and material***

Besides finding that Mn was largely associated with submicrometer particles, we also noticed that this association varied by process, indicating that processes with more manganese distributed in small particles may be potentially more dangerous than others. Mild steel base metal was used in both Factory A and B, while stainless steel was used in Factory C.

Consumables used in Factory A and B slightly differed from what used in Factory C. Statistical models that were used in Chapter Two (mixed effect model study) were employed to analyze data from cassette samplers in this study, with a purpose to evaluate how factors such as process type, base metal, consumable, workload and indoor/outdoor might influence Mn air concentration and size distribution. Due to the small sample size, no significant effects were identified. PM and Mn air concentrations were relatively higher in Factory C than in other two factories, and this could be a result of higher work load, as welding was going on 60% of the time during data collection at Factory C while it was 30% - 40% at Factories A and B. Although Mn concentrations were different, comparing impactor data from Factory B (gas metal arc welding on mild steel) with those from Factory C (gas metal arc welding on stainless steel) revealed no differences in Mn size distribution. These preliminary findings are consistent with the finding in the Chapter Two that the base metal had little effect on Mn exposures.

Manganese content in the consumables used in these factories ranged from 0.45% to 1.55%, except the granular flux used by submerged arc welding that contained 32%-38% Mn as MnO. Measurements during submerged arc welding showed less Mn in particles smaller than 0.5 $\mu$ m and more Mn in larger particles compared to the other three processes, a phenomenon that might be explained by high Mn content in the flux. This high Mn content did not result in high Mn air concentrations in our study, which was consistent with the general knowledge that submerged arc welding produces less fume because during welding the arc is completely covered by the flux. Manganese contents in the base metals used in the factories were less than 1%. Compared to high Mn steel and high Mn consumables that contain 15% of Mn, the ranges of Mn in base metal and consumables used in these factories was small. Thus, the effect of Mn content in the material on Mn air concentration and size distribution were expected to be small. Therefore, process was expected to be the main contributor of the variations in Mn size distribution. Plasma arc welding has been considered as less dangerous based on its low fume generation rates. However, our data indicated that this process had the highest Mn percentage of particle mass for particles < 0.5 $\mu$ m (10%); it also had the highest total of manganese mass fraction distributed in this particle size range (97%). Therefore, when particle and manganese exposure levels are comparable to those from other types of processes, plasma arc welding operations may be potentially more hazardous than others. It is similar for gas metal arc welding. Shielded metal arc welding was found to simultaneously have high fume generation rates, high percentage of particle mass distributed in particles smaller than 0.5 $\mu$ m, and high fraction of manganese mass distributed in particles smaller than 0.5 $\mu$ m. It should be evaluated and controlled with high priority.

## **Future Steps**

We propose to assess manganese distributions in welding fumes smaller than 0.1 $\mu$ m using multiple stage impactors with cut points in ultrafine size ranges. Micro-Orifice Uniform Deposit Impactor (MOUDI) 125-NR is one of the options. It provides cut-points at 0.01, 0.018, 0.032, 0.056, 0.1, 0.18, 0.32, 0.56, 1.0, 1.8, 3.2, 5.6 and 10 $\mu$ m. Required sampling flow rate of 10 liter per minute can be achieved by a SKC Leland Legacy pump. Our study indicated that the sampling and the analytical methods had sufficient sensitivity to detect manganese collected by a multi-stage impactor.

We also propose to evaluate a broader range of welding processes to develop profiles of particle and manganese exposures from other common welding practices, including gas tungsten arc welding, flux core arc welding, laser welding and resistance welding that were not investigated in this study.

## References:

- American Welding Society. (1979) Fume and Gases in the Welding Environment - A Research Report on Fumes and Gases Generated During Welding Operations Miami, Florida: American Welding Society.
- Antonini JM. (2006) Potential neurotoxic responses in rats after pulmonary administration of welding fume with varying concentrations of manganese. *Neurotoxicology* **27**: 1163-1163.
- Araujo JA, Nel AE. (2009) Particulate matter and atherosclerosis: role of particle size, composition and oxidative stress. *Particle and Fibre Toxicology* **6**: Article No.: 24.
- AWS. (1979) Fume and Gases in the Welding Environment - A Research Report on Fumes and Gases Generated During Welding Operations Miami, Florida: American Welding Society.
- Brenneman KA, Wong BA, Buccellato MA, Costa ER, Gross EA, Dorman DC. (2000) Direct olfactory transport of inhaled manganese ((MnCl<sub>2</sub>)-Mn-54) to the rat brain: Toxicokinetic investigations in a unilateral nasal occlusion model. *Toxicology and Applied Pharmacology* **169**: 238-248.
- Burgess WA. (1995) Recognition of Health Hazards in Industry; A Review of Materials and Processes. 2nd New York: John Wiley & Sons. ISBN 0 471 57716 2.
- Ellingsen DG, Hetland SM, Thomassen Y. (2003) Manganese air exposure assessment and biological monitoring in the manganese alloy production industry. *Journal of Environmental Monitoring* **5**: 84-90.
- Iregren A. (1990) PSYCHOLOGICAL TEST-PERFORMANCE IN FOUNDRY WORKERS EXPOSED TO LOW-LEVELS OF MANGANESE. *Neurotoxicology and Teratology* **12**: 673-675.
- Lippmann M, Chen LC. (2009) Health effects of concentrated. ambient air particulate matter (CAPs) and its components. *Critical Reviews in Toxicology* **39**: 865-913.
- Madl AK, Pinkerton KE. (2009) Health effects of inhaled engineered and incidental nanoparticles. *Critical Reviews in Toxicology* **39**: 629-658.
- Samuelsen M, Nygaard UC, Lovik M. (2009) Particle Size Determines Activation of the Innate Immune System in the Lung. *Scandinavian Journal of Immunology* **69**: 421-428.
- Santamaria AB, Cushing CA, Antonini JM, Finley BL, Mowat FS. (2007) State-of-the-science review: Does manganese exposure during welding pose a neurological risk? *Journal of Toxicology and Environmental Health-Part B-Critical Reviews* **10**: 417-465.
- Schmid O, Moller W, Semmler-Behnke M, Ferron GA, Karg E, Lipka J, et al. (2009) Dosimetry and toxicology of inhaled ultrafine particles. *Biomarkers* **14**: 67-73.
- Tjalve H, Henriksson I. (1999) Uptake of metals in the brain via olfactory pathways. *Neurotoxicology* **20**: 181-195.

Figure 1 Cumulative distribution plots for total and respirable PM and Mn

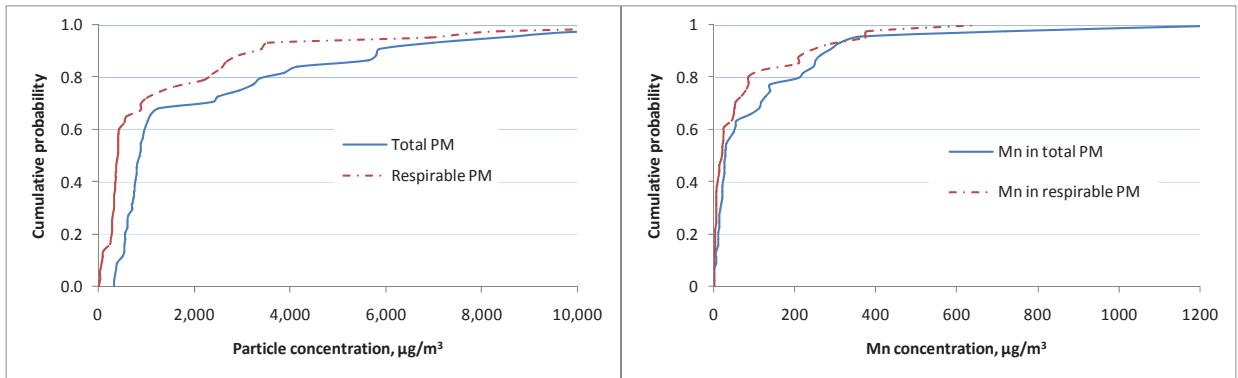


Figure 2 PM and Mn concentrations by processes,  $\mu\text{g}/\text{m}^3$

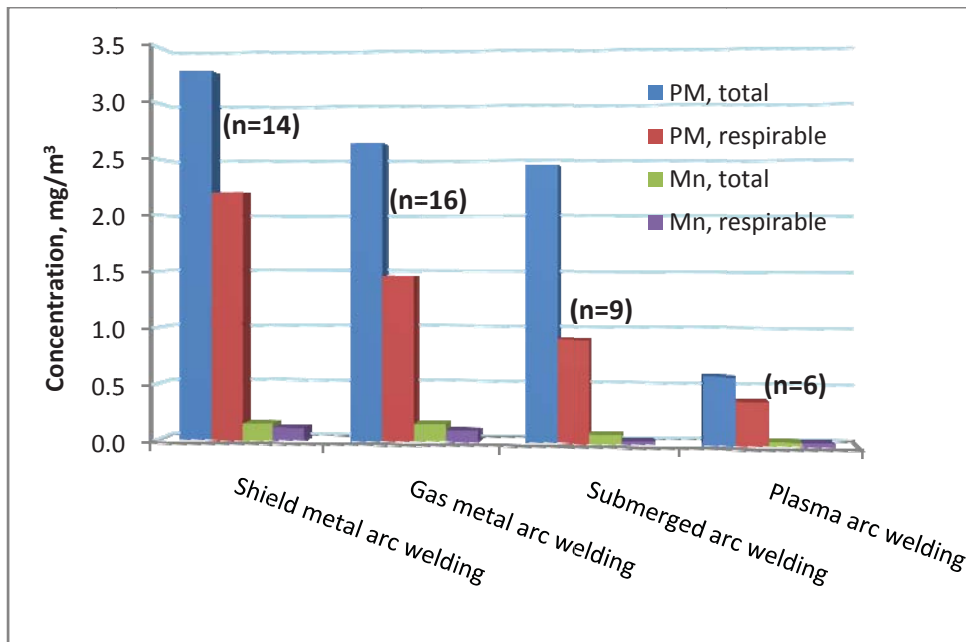


Figure 3 Particle and Mn exposures by factories

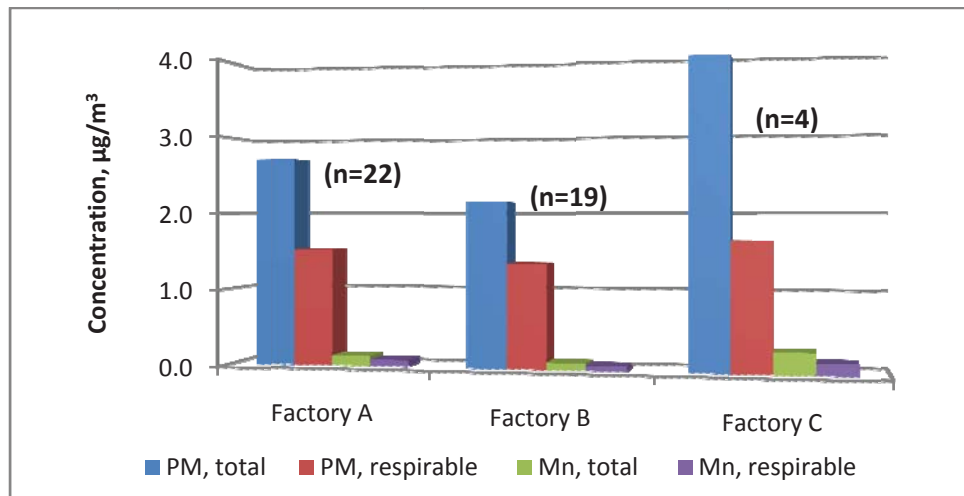


Figure 4 PM and Mn mass distributions by processes (percentage of total mass of PM and Mn in each particle size range)

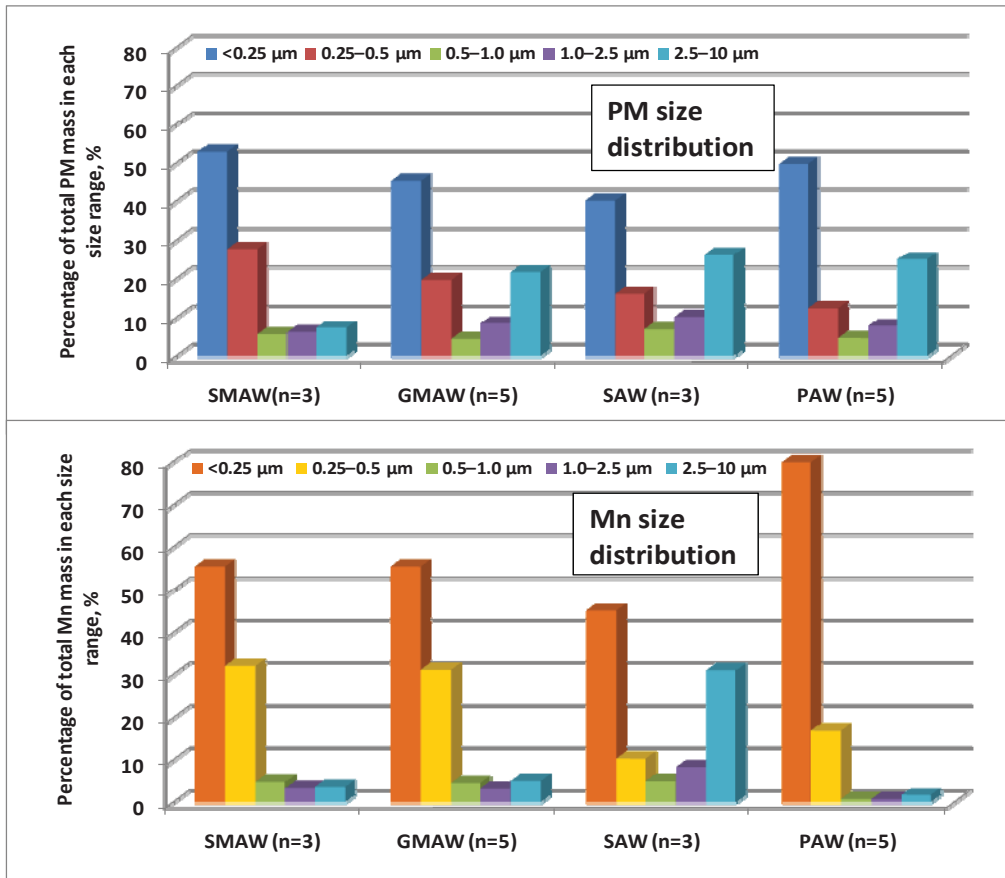


Table 1 Fume generation rates when mild steel is welded using SMAW or GMAW and selected electrodes (American Welding Society, 1979)

Process type	Electrode classification	Current range A	Fume generation rate, g/min
Shielded metal arc welding (covered electrode)	E6010	140-150	0.83
	E6013	145-160	0.31-0.58
	E7018	170-180	0.57-0.60
	E7024	200-230	0.43-0.55
	E8018 C3	160-175	0.43-0.47
	E9018 B3	160-180	0.36-0.46
Gas metal arc welding (solid electrode)	E70S-3	260-290	0.41-0.46
	E70S-5	275-290	0.38

Table 2 Sample collection summary

Factory	Day	Welding process type			
		Shield metal arc welding	Gas metal arc welding	Submerged arc welding	Plasma arc welding
Factory A	Day 1	4 pairs of total/respirable (1 breathing zone + 3 area); 1 impactor (breathing zone)		2 pairs of total/respirable (1 breathing zone + 1 area); 1 impactor (breathing zone)	
	Day 2	4 pairs of total/respirable (1 breathing zone + 3 area); 1 impactor (breathing zone)			2 pairs of total/respirable (1 breathing zone + 1 area); 1 impactor (breathing zone)
	Day 3	4 pairs of total/respirable (1 breathing zone + 3 area); 1 impactor (breathing zone)			3 pairs of total/respirable (1 breathing zone + 2 area); 1 impactor (breathing zone)
	Day 4	2 pairs of total/respirable (area)		2 pairs of total/respirable (breathing zone); 2 impactor (breathing zone)	
	Day 5				1 pair of total/respirable (breathing zone)
Factory B	Day 1	1 pair of total/respirable (area)	3 pairs of total/respirable (1 breathing zone + 2 area); 1 impactor (breathing zone)	1 pair of total/respirable (breathing zone); 1 impactor (breathing zone)	
	Day 2	1 pair of total/respirable (area)	3 pairs of total/respirable (1 breathing zone + 2 area); 1 impactor (breathing zone)	2 pair of total/respirable (1 breathing zone + 1 area); 1 impactor (breathing zone)	
	Day 3	1 pair of total/respirable (area)	3 pairs of total/respirable (1 breathing zone + 2 area); 1 impactor (breathing zone)	2 pair of total/respirable (1 breathing zone + 1 area); 1 impactor (breathing zone)	
Factory C	Day 1		4 pairs of total/respirable (2 breathing zone + 2 area); 2 impactor (breathing zone)		
Total	9 days	17 pairs of total/respirable (3 breathing zone + 14 area); 3 impactor (breathing zone)	13 pairs of total/respirable (5 breathing zone + 8 area); 5 impactor (breathing zone)	9 pairs of total/respirable (6 breathing zone + 3 area); 6 impactor (breathing zone)	6 pairs of total/respirable (2 breathing zone + 4 area); 2 impactor (breathing zone)

Table 3. Process characteristic information planned to be gathered

---

Process type: SMAW, GMAW, SAW, PAW

Welding material

Base metal classification number  
Consumable classification number

Operation parameters

Automatic / manual operation  
Current range, in ampere (A); Current density, in A/mm  
Voltage, in volt  
Welding speed, in mm/second; Wire feed rate, in mm/second

Work load/welding rate

Duty cycle (% of welding time)  
Wire/rod consumption rate (kg/day)

Work environment conditions

Indoor / outdoor  
Confined space / open space  
Local exhaust ventilation, mechanical ventilation / general ventilation

---

Table 4 Summary statistics for particle and manganese exposures, mg/m<sup>3</sup>

	<u>PM</u>		<u>Mn</u>	
	<u>Total (n=43)</u>	<u>Respirable (n=42)</u>	<u>Total (n=43)</u>	<u>Respirable (n=40)</u>
Arithmetic mean	2.58	1.46	0.122	0.073
Standard deviation	4.52	2.68	0.227	0.132
Coefficient of variation	175%	183%	186%	180%
Range	0.338 – 27.8	0.011 – 14.7	0.001 – 1.30	0.001 – 0.650
Geometric mean	1.28	0.698	0.058	0.036
Geometric standard deviation	3.27	3.37	3.40	3.33

Table 5 Particle size distribution, as ratio of respirable particle air concentration to total particle air concentration, and percentage of particle mass distributed in particles <0.5µm, averaged over factories

<u>Process</u>	Ratio, respirable conc. <u>/total conc. (n)</u>	% of PM mass distributed <u>in particles &lt;0.5µm (n)</u>
Shielded metal arc welding	0.67 (14)	0.81 (3)
Gas metal arc welding	0.55 (16)	0.65 (5)
Submerged arc welding	0.37 (9)	0.56 (3)
<u>Plasma arc welding</u>	<u>0.65 (6)</u>	<u>0.62 (5)</u>
Average	0.56 (45)	0.66 (16)

Table 6 Mn size distribution, as ratio of Mn air concentration in respirable particles to those in total particles, and percentage of Mn mass distributed in particles <0.5µm, averaged over factories

	Ratio, Mn in respirable PM /Mn in total PM (n)	% of total Mn mass distributed in particles <0.5µm (n)
Shielded metal arc welding	0.75 (14)	0.88 (3)
Gas metal arc welding	0.62 (16)	0.87 (5)
Submerged arc welding	0.27 (9)	0.55 (3)
<u>Plasma arc welding</u>	<u>0.86 (6)</u>	<u>0.97 (5)</u>
Overall	0.63 (45)	0.82 (16)

Table 7. Percentage of particle mass composed of manganese, by particle size ranges and processes

<u>Size</u>	<u>SMAW (n=3)</u>	<u>GMAW (n=5)</u>	<u>SAW (n=3)</u>	<u>PAW (n=5)</u>
<0.25 $\mu\text{m}$	5.3	6.4	4.5	10.7
0.25–0.5 $\mu\text{m}$	5.4	5.9	2.3	10.2
0.5–1.0 $\mu\text{m}$	3.9	2.8	2.2	1.4
1.0–2.5 $\mu\text{m}$	2.5	1.9	2.1	0.6
2.5–10 $\mu\text{m}$	2.0	1.2	3.2	0.4

## Conclusions

Welding is a process that is widely used in a variety of industrial settings. It is estimated that there are 1 million full-time and 5 million part-time welders worldwide. There may be more workers who do some welding as a part of their job but are undeclared as part-time welders. Moreover, by-standers at a welding workplace may also get exposed even if they do not perform welding tasks. Therefore, the number of exposed workers may be even larger. Welding fumes are known to be toxic. Welders' exposures to welding fumes are difficult to assess because they are highly variable. Although many studies have been conducted in experimental settings to evaluate the associations between fume exposures and process conditions, such as how fume generation rates are affected by process operation parameters, details are not well known as to how the exposures may vary in practice and what the exposure determinants are. This dissertation was conducted to address these issues to gain better understanding of the exposures to welding fumes.

From the research presented in the previous chapters the following conclusions are made: exposures to particulate matter (PM) and Manganese (Mn) in welding fumes vary considerably across the world and across occupational groups. Exposures to both contaminants have been and continue to be unacceptably high in many sectors of industry. Important exposure determinants were identified in this dissertation work. Due to the fact that the two agents have different determinants, separate control strategies should be developed and used for reducing welders' exposures to PM and Mn. It was observed that exposures in a given facility varied substantially over space and time. Particle size distributions and Mn distribution in different size of particles were found to be important aspects of welding fume exposures. Therefore, variations (spatial and temporal) and size characteristics (of PM and Mn) need to be considered in developing exposure assessment and control strategies.

First, exposures to welding fumes, as represented by total particulate matter (TP) and Mn, were observed to be high and unchanged over the past 40 years. In the mixed effect model study, the overall arithmetic mean (AM) was  $4.79 \text{ mg/m}^3$  (range:  $0.001 \text{ mg/m}^3$  to  $251 \text{ mg/m}^3$ , GM:  $1.81 \text{ mg/m}^3$ , GSD: 4.04) and  $0.502 \text{ mg/m}^3$  (range:  $0.001 \text{ mg/m}^3$  to  $16 \text{ mg/m}^3$ , GM:  $0.160 \text{ mg/m}^3$ , GSD: 4.54) for TP and Mn in TP, respectively. Using  $5 \text{ mg/m}^3$  for TP and  $0.2 \text{ mg/m}^3$  for Mn in TP as operative OELs, the AMs were 95.5% and 2.5-folds of the respective OELs. The study further found that the estimated probabilities of exceeding OELs were unacceptably large for both TP and Mn. Estimates of exceedances and probabilities of overexposure were greater than 0.10 for all countries, except for TP exposures in the U.K., and for all industries, except for TP exposures in the automobile assembly industry. Estimated exceedances and probabilities of overexposure were much greater for Mn than for TP exposures. Exposure to Mn in the U.S. had an estimated exceedance of 35% and an estimated probability of overexposure of 51%. Mn exposures in the railroad industry were estimated to have an exceedance of 66% and a probability of overexposure of 87%. If a new TLV of  $0.02 \text{ mg/m}^3$  for Mn in respirable particulate matter were to take effect, our results suggest that it would be exceeded in virtually all welding operations, with exceedances ranging from 56% to 96% and probabilities of overexposure ranging from 79% to 100%, given welding fumes are predominantly respirable particles.

These findings are particularly troubling in light of the fact that we detected no trend towards reduction in exposure to TP and Mn in welding operations over the past 40 years,

running counter to the consistent reductions in air levels of most chemical agents that have been well documented over a similar time period. High levels of exposures to PM and Mn in welding fumes were also observed in exposure data collected in three Chinese factories (“Mn size distribution study”). The overall AMs for TP and Mn in TP (8-hr TWA) across processes and factories were 2.58 mg/m<sup>3</sup> (range: 0.338 mg/m<sup>3</sup> – 27.8 mg/m<sup>3</sup>, GM: 1.28 mg/m<sup>3</sup>, GSD: 3.27) and 0.122 mg/m<sup>3</sup> (range: 0.001 mg/m<sup>3</sup> – 1.30 mg/m<sup>3</sup>, GM: 0.058 mg/m<sup>3</sup>, GSD: 3.40), respectively. Over 20% of measurements for TP and Mn in TP exceeded Chinese respective OELs. The overall AMs for respirable PM and Mn in respirable PM were 1.46 mg/m<sup>3</sup> (range: 0.011 mg/m<sup>3</sup> – 14.7 mg/m<sup>3</sup>, GM: 0.698 mg/m<sup>3</sup>, GSD: 3.37) and 0.073 mg/m<sup>3</sup> (range: 0.001 mg/m<sup>3</sup> – 0.650 mg/m<sup>3</sup>, GM: 0.036 mg/m<sup>3</sup>, GSD: 3.33), respectively. Eighteen percent and 52% of measurements for respirable particles and Mn in respirable particles exceeded the current TLV of 3 mg/m<sup>3</sup> for respirable PM and proposed TLV of 0.02 mg/m<sup>3</sup> for Mn in respirable PM. These data indicated that exposures to both PM and Mn in these factories might be high enough to be of concern.

Second, exposures to welding fumes vary substantially across the countries and occupational groups. In the mixed effect model study, exposures to TP varied more than six orders of magnitude from 0.001 mg/m<sup>3</sup> to 251 mg/m<sup>3</sup>, with a coefficient of variation of 2.46 (AM = 4.79 mg/m<sup>3</sup> and SD = 11.8 mg/m<sup>3</sup>); exposure to Mn in TP varied more than five orders of magnitude from 0.001 mg/m<sup>3</sup> to 16 mg/m<sup>3</sup>, with a coefficient of variation of 2.97 (AM = 0.502 mg/m<sup>3</sup> and SD = 1.49 mg/m<sup>3</sup>). The geometric standard deviations (GSDs) for exposures to both agents were greater than 4.0, at the high end of GSDs that are usually observed in occupational exposures. The country, industry/trade, workplace configuration (open space vs. enclosed space) and ventilation were identified as the major common factors affecting exposures to both TP and Mn. Base metal, welding process and trade appeared to have significant effects on TP exposures, while Mn exposures were mainly driven by the consumable and the type of work. Base metal and welding process did not have noticeable effects on Mn exposures (except resistance welding). When these factors were controlled, variance components between groups and between individual workers within a group were reduced by 89% and 57% for TP, and 75% and 63% for Mn, respectively. However, within-worker variations in Mn exposures appeared to be three times higher than those in TP exposures, indicating individual worker’s exposure to Mn varied substantially over time (within a day and from day to day) and exposures to TP and Mn had different determinants. These variations and determinants are important in exposure assessment and control.

Moreover, considerable temporal and spatial variations were observed at the automobile assembly facility in the PM mapping study. Particulate matter air concentration at fixed locations varied 21%-30% over a shift, as measured by 1-minute TWAs. The coefficients of variation were larger if the concentrations were measured in shorter sampling durations. Although these variations did not seem very large, they had profound effects on PM mapping. The map of particle mass concentration revealed several high concentration areas, requiring further investigation and potentially higher level of controls. Using overall arithmetic spatial means across 212 locations as surrogates of the spatial distributions, repeated ANOVA analysis revealed that particle spatial distribution varied significantly across six sampled days, indicating a need for repeated measurements. Mapping was demonstrated to be an effective method to assess particle spatial distributions. A careful evaluation of temporal variations is essential in developing mapping protocols. As indicated by the PM mapping study, failure to capture

temporal variations resulted in the data collected by the facility EHS personnel being insufficient to evaluate the reduction of the particle concentrations after the countermeasures.

Third, particle size characteristics are important aspects of welding fume exposures. In the PM mapping study, the map of submicrometer particle count concentration (0.014 $\mu\text{m}$  to 1.0 $\mu\text{m}$ ) presented different patterns from that of respirable particle mass concentration. The map of submicrometer particle count concentration had a smaller spatial gradient, indicating that submicrometer particles are both more readily transported with air currents and less likely to settle, and thus more uniformly distributed in a facility. Therefore, workers not in close proximity to intensive welding operations might be exposed to fine particles at levels higher than had traditionally been thought. Size characteristics become more important in exposures to Mn. In the Mn size distribution study, Mn was found to be more concentrated in respirable particles than in total particles. Data from the multi-stage impactors revealed that both Mn mass fraction (of total Mn mass) and percentage of particle mass contributed by Mn increased substantially in particles smaller than 0.5 $\mu\text{m}$ . This finding is of great significance in that Mn primarily targets the central nervous system and small particles in the nano-size range may reach the brain via olfactory transportation bypassing the blood-brain barrier. Inhaled nano-size particles also can penetrate into the blood stream and thus might potentially be transported into the brain. Mn in small particles may also have higher bio-availability due to larger surface area of small particles. Therefore, welders' risk of developing neurological effects due to exposures to Mn may be potentially higher than it had been thought. Welding processes generate particles with more Mn distributed in fine and ultrafine particles and so are potentially more hazardous than other processes.

Lastly, control strategies need to be developed that are customized for specific contaminants in welding fumes, with considerations of potential exposure determinants, exposure variations, and particle size specifics. The mixed effect model study established that exposures to TP and Mn were affected by different determinants. While base metal and trade appeared to have more influence on exposures to TP, exposures to Mn were more affected by composition of consumable materials and type of hot work (see Chapter Two). Separate control strategies are needed to reduce exposures to TP and Mn. Also, in the mixed effect model study local exhaust ventilation (LEV) was found to be very effective in controlling the exposures. However, in the PM mapping study at the automobile assembly facility LEV was found not to function equally well for all size particles. Enclosed and vented processes were found to be more effective in capturing larger particles, while a significant fraction of small particles, especially submicrometer particles, were still emitted from the processes into the facility and thus particle distribution was shifted to smaller particles. These findings indicate that ventilation needs to be designed and evaluated by the reductions not only of mass concentrations but also of count concentrations for small particles, especially for welding processes that are known to generate fine and ultrafine particles. Moreover, the mixed effect study found that resistance welding generally produced significantly lower TP and Mn exposures compared to other welding processes, and that the concentrations were lower in automotive manufacturing. However, the PM mapping study at an automotive assembly plant suggested that resistance welding operations could still be major particle emitting sources in a facility if not effectively controlled. These findings emphasize that emissions from less hazardous welding operations such as resistance welding should also be effectively controlled. Therefore, removal of fine and ultrafine particles from a facility is more important than blowing them away from the emission sources. Exposures

of those who do not work in the close vicinity of the emission sources should also be evaluated when assessing workers' exposure to fine and ultrafine particles.

## **Future Steps**

In this dissertation, three research projects were conducted to gain knowledge of the wide range of welders' exposures to PM and Mn, the exposure determinants, and the size characteristics of PM and Mn in welding fumes. Our data revealed that Mn was not evenly distributed across the size ranges measured by the cassette samplers or the multiple-stage impactors. Due to limited resources, manganese distribution in ultrafine particles was not measured. Given the potential contribution of Mn in ultrafine particles to toxicity, we propose to assess manganese distributions in welding fumes smaller than 0.1  $\mu\text{m}$  using multiple-stage impactors with cut points in ultrafine size ranges.

We also propose to evaluate a broader range of welding processes. Several important common welding processes that were not investigated in this study include gas tungsten arc welding, flux core arc welding, laser welding and resistance welding, among which flux core arc welding is known to have high potential of manganese exposure. By evaluating particle and manganese exposures for a wide range of common welding processes, with an emphasis on manganese size distribution, we expect to develop profiles of particle and manganese exposures for common welding practices. When the base metal was similar, operational parameters were also similar for a given process across welding sites and factories. Consumables and the operational parameters appeared to be chosen following certain standard guidelines to achieve optimal welding outcomes. This finding makes it possible to profile the PM and Mn air concentrations produced by common welding process under common operational conditions. Information on materials commonly used, operational parameters, application environmental conditions and other relevant factors can be retrieved from American Welding Society publications. The developed profiles can be used to help us better understand the range of welders' exposure to particles and manganese, especially manganese in ultrafine particles. These profiles can further be used to plan exposure assessment in epidemiological studies to assign/select homogenous exposure groups, to estimate exposures for risk assessment of welders' exposure to welding fume and manganese, and to guide control measures.